One Hundred Channel Electrophoresis Prototypes for Application to an Ultra-High Throughput Mutational Spectrometer

By

Michael J. Beltran

SUMBITTED TO THE DEPARTMENT OF MECHANICAL ENGINEERING IN PARTIAL FULFULLMENT OF THE REQUIREMENTS FOR THE DEGREE OF

BACHELOR OF SCIENCE IN MECHANICAL ENGINEERING
AT THE
MASSACHUSETTS INSTITUTE OF TECHNOLOGY

JUNE 2007

Signature of Author: _____
Department of Mechanical Engineering
May 11, 2007

Certified by: _____
Ian W. Hunter
Hatsopoulos Professor of Mechanical Engineering
Thesis Supervisor

Accepted by: _____
John H Lienhard
Chairman of the Undergraduate Thesis Committee, Professor of Mechanical Engineering

One Hundred Channel Electrophoresis Prototypes for Application to an Ultra-High Throughput Mutational Spectrometer

By

Michael J. Beltran

Submitted to the Department of Mechanical Engineering
On June 8, 2007 in Partial Fulfillment of the
Requirements for the Degree of Bachelors of Science in
Mechanical Engineering

ABSTRACT

Mutation detection within the human genome is becoming an increasingly important field today. It is possible that with a correlation between diseases and the mutations that cause them, new therapeutic treatments could be developed against many of today's common diseases In order to accomplish mutation detection, 10^{12} gene segments may be needed, requiring a significant increase in current technologies An instrument termed an Ultra-high throughput mutational spectrometer (UTMS) uses a process known as constant denaturing capillary electrophoresis (CDCE) to detect mutations in 10,000 capillaries simultaneously. The UTMS is at a 100-capillary proof of concept stage to successfully perform CDCE. In order for this stage to be successful, multiple subsystems of the device must work in unison, including thermal control, optical detection, electrical and fluidic connectivity. In this thesis, multiple devices were created to work in conjunction with previously existing instruments, including a passively aligned 100-port buffer reservoir and DNA injection loading plate. These devices were used to perform electrophoresis on DNA fluorescent primers in order to test the functionality of the UTMS 100-stage concept. A procedure for performing these experiments was developed in order to minimize risk and maximize chance of success. Successful isolation of individual signal detection was accomplished through the use of these procedures and devices, proving the 100-capillary proof of concept may reliably and repeatedly perform CDCE on the UTMS.

Thesis Supervisor: Ian W. Hunter

Title: Hatsopoulos Professor of Mechanical Engineering

Acknowledgements

I would firstly like to thank Professor Ian Hunter for allowing me to conduct my thesis research in the BioInstrumentation lab. The experience and knowledge I have gained from such a rich surrounding will be of unparalleled use to me in the future, and I will never forget the time I have spent working with some of the brightest at MIT in one of the best laboratories.

Secondly, I would like to thank Craig Forest for his guidance and mentorship through my senior year at MIT, and Miguel Saez for help as a fellow undergraduate. Finally, all three of us can graduate.

Lastly, I would like to extend to my parents a thank you which no words can describe. You have lived the American dream, and have given me the opportunities you never had as children. I promise to make the most out of everything you have given me.

Table of Contents

Table of Figures

1.0 Introduction

Mutation detection in the human genome has become an increasingly important field because of the impact it may have on the future of medicine. Genetic mutations are responsible for many of the common diseases that affect humans today, but very little is known of the complex nature of the mutations that cause the disease. Methods that currently exist today are limited by the amount of throughput, where detection of mutations would require a 2-3 order of magnitude increase in existing technologies. The goal of this research is to create an "Ultra-high mutational spectrometer" (UTMS) which is capable of sorting through the required 10^{12} gene fragments to statistically correlate mutations and disease [17]. With these genetic markers for disease, new tests can be developed to identify risk and be used to develop preventative or therapeutic treatments [2]. The throughput necessary to achieve this correlation is possible with a 10,000 capillary array in the UTMS which will be able to sort through 1 million separate person's DNA in approximately 30 minutes. With this level of throughput, it will be possible to correlate approximately 100 common diseases to their corresponding genetic markers within a two year period.

2.0 DNA and Mutations

Deoxyribonucleic Acid, commonly known is DNA is the molecule responsible for communicating all the instructions necessary to create a human being. Each protein within the human body is created off of this template, and it is responsible for the huge differences between humans and a frog, as well as the minute variations between a blonde and brown haired human child. DNA forms what can be thought of as a blueprint for life, made up of four different molecules called bases: Adenine, Thymine, Cytosine, and Guanine, which pair with one another;

Adenine to Thymine, and Cytosine to Guanine (A-T, G-C) [3]. In a normal cell, proteins are transcribed from these patterns of pairs. However, there are situations when this transcription may not proceed as intended, because of an unintended change in the DNA base pairing. This change, or mutation, could be the result of one of many spontaneous or induced reasons, and can cause the incorrect transcription of proteins from DNA. While this is the same mechanism that is responsible for evolution of life, it is also the mechanism which causes many diseases common to man today. Consequently, a person with a certain genetic disease faces the risk of passing his or her genetic mutation to their offspring, as a child is the combination of genetic material from both the mother and father. This child now may run the risk of the same disease, and face the same risk of passing it to his or her own offspring [3].

2.1 Mutation Detection

The UTMS project is seeking to be able to detect these mutations within an individual's genetic makeup, in order to correlate to those diseases which result from the mutations. Currently, there are many methods available to detect a mutation within a genetic segment. However, an incredibly high throughput is necessary to be able to detect mutations within an entire human's genetic material, because each human genome contains approximately 3×10^9 bases. While the DNA replication process has its own repair enzymes which can replace translation mistakes [3], it can still miss a mutation. As a result, the percentage of mutations within the human genome is well below the fractions of a percent [4]. To be able to detect this low percentage of mutations, an incredibly high-resolution scanning method is necessary to be able to identify these segments. One such process is termed Denaturing Gradient Gel Electrophoresis (DGGE) [5].

Simple DNA electrophoresis is accomplished by placing single stranded DNA within a viscous polymer matrix, and drawing the segments across the gel medium by a potential voltage. Due to the negative charge of a single stranded DNA segments, the segments of DNA will be drawn to the cathode, or positive side of the voltage potential. These DNA segments vary in length, and are forced to make their way through the gel matrix in order to reach the cathode. Thus, larger segments will have a harder time working their way through than the smaller segments. A spatial gradient thus emerges, and segments can be distinguished and separated based on their lengths.

While simple electrophoresis can distinguish only between single stranded segments with difference in lengths, Denaturing Gradient Gel Electrophoresis has the capability to distinguish between double stranded mutant and wild-type segments of equal base pair length. In normal wild-type DNA, the bonds between each base pair may be broken if the sample is heated, causing double stranded DNA to break down to two single strands. [3] However, in mutant DNA, the temperature required to break the base pair bonds is less than that of the wild type DNA because of the weaker bond in the mismatched pair. Hence, if a mixture of wild-type and mutant DNA is brought to a temperature above the mutant requirement to denature, but below the wild type requirement, only the mutant segment will undergo an "unzipping", where the weak point in the segment will cause the DNA to spread open from that point towards the end of the segment [5]. The "arms" of the DNA will thus inhibit its flow through a gel matrix, much similar to the effect a larger segment of DNA would have a more difficult time navigating a gel medium compared to a shorter one [3]. The differing migration bands may be observed visually by attaching a phosphorescent primer to each of the segments of DNA, the resultant spatial

gradient can be observed by the naked eye. Figure 1 below illustrates a gradient shown illuminated in gel:

Figure 1: Spatial gradient between wild type and mutant DNA segments with phosphorescent illumination. Taken from [6].

Yet another improvement in electrophoresis comes in the form of Constant Denaturing Capillary Electrophoresis (CDCE) [5]. Electrophoresis is instead performed in a fused glass silca capillary with a small inner diameter (~75 μm), filled with a viscous fluid. This method is much quicker because of multiple reasons, including the small mass of gel necessary for an experiment, as well as higher voltage each capillary is capable of, allowing electrophoresis to proceed quicker than across a gel slab. Additionally, because of the small thermal mass of each capillary, precise temperature control can be maintained, which is a critical component of denaturing electrophoresis. Rather than guess an experimental temperature and observe the spatial difference between segments, a precise temperature can be selected and the separation of wild-type and mutant DNA can be observed through time [5]. Each DNA fragment is labeled with a phosphorescent molecule as it is in DGGE, and is observed passing through a fixed point

in each capillary. The fluorescence will thus be typically observed in 4 distinct signal peaks – two homoduplexes (Both strands of the double helix are either wild-type or mutant), and two heteroduplexes (one strand of the double helix is wild-type, the other is mutant). These segments can also be predicted to reach a fixed point in a certain order because of the nature of their denaturing. The wild type homoduplex will arrive first, followed by the mutant homoduplex (double helix will not denature because there is no incorrect base pairing), and next by the heteroduplexes (which will have denatured and unzipped), causing them to move much slower than the homoduplexes. Below is a signal graph representing the separation and intensity of each type of DNA segment in CDCE.

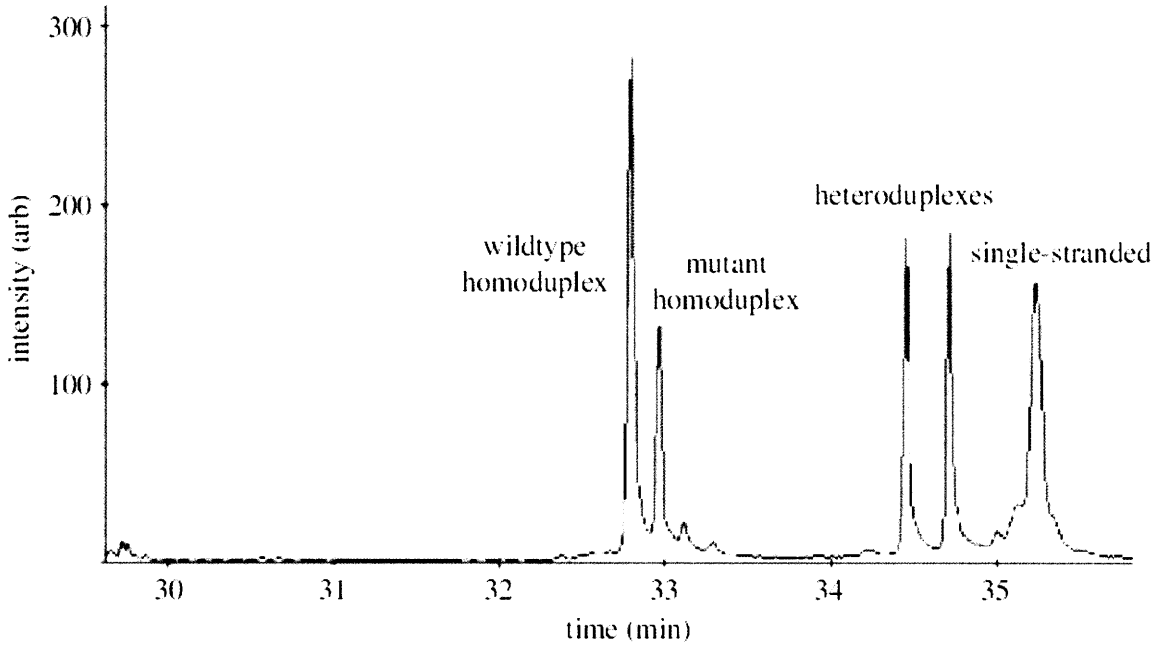

Figure 2: CDCE time separation gradient showing heteroduplex, homoduplex, and primer separation. Taken from [7].

Another advantage to CDCE is the capability to run multiple channels at once, even without knowing which is mutant and which is wild-type. The first to appear will be the wild-type DNA, allowing a distinction to be made between the two previously unknown samples. This

concept is critical to mutation analysis, since it does not require a selection based on phenotype prior to experimentation.

2.2 Mutational Spectrometry

CDCE provides an excellent method to separate mutant from wild-type DNA, creating a spectrum of data that can be used to correlate specific single or multi-allele mutations with their corresponding diseases [9]. The key aspect of CDCE is the non-requirement of previous phenotypic selection; there needs to be no previously known trait that distinguishes wild-type from mutant in a person [8]. Thus, mutated DNA can be identified in persons who exhibit no differing traits. It is thus possible to gather data on millions of people and compare their DNA to scan for mutations. A correlation can thus be developed between the mutational scan, and the phenotypes exhibited, and the suspect mutation can be identified [9].

3.0 Ultra-high throughput mutational spectrometer (UTMS)

A massive amount of data is necessary to be able to quantify mutations across the human genome, and identify the corresponding resultant diseases. It is required that 10^{12} gene fragments be scanned, as outlined by *Morgenthaller et al* [17]. There currently exists machines which may allow a few hundred channels to be run simultaneously, but with current technology the time required to scan the required number of genes is beyond the hundreds of years. An instrument is needed to be able to be able to scan a massive amount of data within a reasonable time period to provide quick results for populations study. The goal of this project is to construct such a machine which will be able to scan 10,000 separate channels within a 30 minute time frame,

requiring 1 million different person's DNA to run at once. The data collected within two years of operation of such a machine will yield the required data to correlate a disease to its genetic cause.

The approach taken in the creation of this instrument has been to separate the development into three stages; single capillary, 100 capillary, and 10,000 capillary detection. At each stage, the methods to be used in the final stage are verified, and will then be scaled to the next stage with development of all necessary tools, with purpose being to identify and solve all problems with massive array detection at the 100 capillary level before committing the time and resources that will be necessary at the 10,000 capillary level. As of the publication of this thesis, there has been successful mutation detection using the instrument outlined in Forest *et al* [1], using side column detection. The procedures and requirements have been successfully transferred to the UTMS, where successful end-column detection has taken place using the same parameters as side-detection. The following steps are to thus create the necessary instruments to scale to the 100-capillary stage of development.

3.1 Required subsystems

In order to accommodate a 100-capillary array, the UTMS requires an integration of multiple subsystems, including thermal control, optical detection, capillary array constraint, gel injection, and electrical systems. As of the time of this publication, there has been large progress towards completion of the mentioned systems, with many of the necessary subsystems created in previous theses. It is the goal of this thesis to integrate the existing tools that have been previously created with the remaining required instruments to be developed, and achieve successful 100-column DNA detection.

3.1.1 Existing tools

The instruments which have been completed include the following; Thermal control chamber, gel loader, capillary array constraint device, and optical detection system.

The thermal control unit makes up the bulk of the existing UTMS, and has thus required the most modification to integrate the system into the full instrument. The device as initially constructed is outlined in Timothy Suen's MIT Bachelors of Science thesis [16], and has been shown to be able to control a simulated heating input to within the requisite ±0.2 °C. The unit requires interfaces to many of the other systems, including gel injection, and capillary constraint. Both are taken into account within this design, and have been shown to accommodate these systems, which will be discussed in detail later in this chapter. The main modification to this device has been the disassembly of its stand, and the integration of the chamber into the main chassis of the UTMS. Sliding bearing and bearing rails were designed to allow a loading position where the instrument could be prepared for an experiment, and a detection position where the entire assembly could be moved to allow for optical detection. The bearing and bearing rails were designed to minimize deflection and angular displacement at the center of the beams, in order to keep the top of the 100-capillary array on a horizontal detection plane. The bearing rails were sized according to the simple beam bending equation for 3-point loading on a beam, as shown:

$$\delta = \frac{FL^3}{48EI},$$

where δ is deflection, F is applied force at the center of the beam, L is the length of the beam, E is modulus of elasticity, and I is the polar moment of inertia. Required beam diameter was calculated to be approximately 0.16 m. A detailed design description can be found in Appendix

A. The following photograph shows the completed extended frame and incorporation of the bearing system;

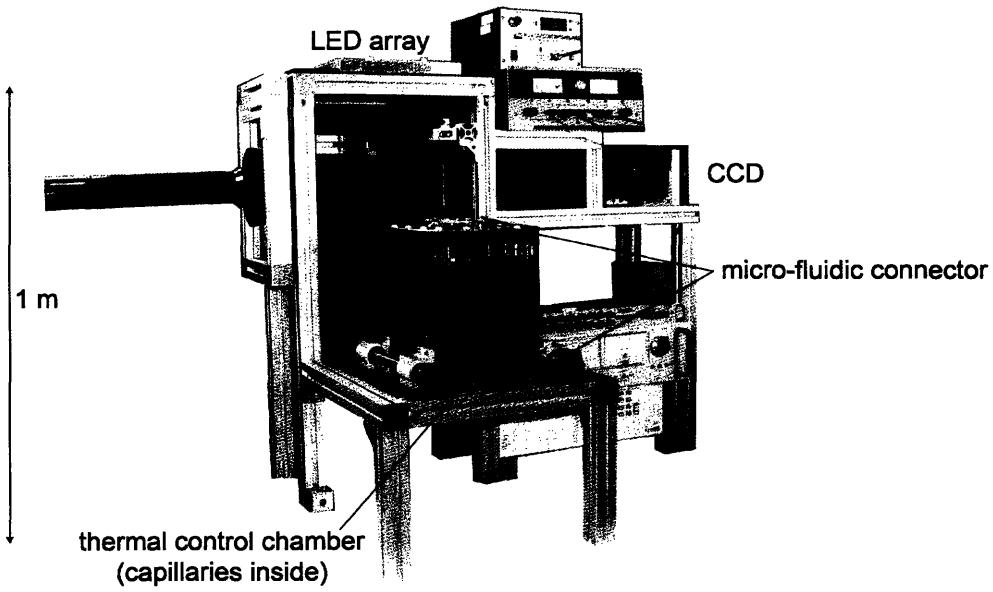

Figure 3: Extended UTMS structure with bearing integrated thermal control chamber.

The gel injection device is explained in detail in Nathan Ball's MIT Senior thesis [12]. The Gel loading device has been show to successfully integrate to the bottom of the thermal control unit, and has successfully injected polyacrylamide gel into all 100 capillaries in the array. Experimental data has shown that on average the capillaries should take just under 30 seconds to completely load, however within recent experiments a much lower standard deviation has been observed, however not quantified. None the less, the gel loader performs above expectations and allows for reasonably quick and simple gel loading procedures. The gel loader has also been adapted for use in an additional step regarding the buffer reservoirs necessary on the top end of the capillary array. This function will be discussed in greater detail in the sections describing the second iterations of buffer reservoir design and procedure.

The capillary array constraint device is the device used to constrain the capillaries at the top and bottom of the thermal control chamber. The device design and construction is described in Forest *et al* [13]. Currently, the device has performed as expected, however there have been a large number of small issues that have arisen with the capillary constraint device, most often resulting in incorrect alignment with regards to the buffer reservoirs, which will be discussed in greater detail in the 1st iteration section on design of the buffer reservoirs. As so far, the greatest challenge in using the capillary constraint device has been to secure a method to assemble and safely insert the array into the thermal chamber. Outlined below is a procedure that has been repeatedly tested to ensure safe insertion. Note that two persons are required to perform the operations safely:

1) Capillaries should be inserted into both loosened upper and lower constraint devices in the prescribed bed plate as described in Forest *et al.* [13]. Marked corners should be aligned to ensure coordinate zero's match to the heat exchanger.
2) Bottom capillaries should be set to 6mm using prescribed alignment push plate and appropriate spacers, and tightened to full.
3) Top capillary constraint device should be pulled to within 30mm of the top of the capillaries, and placed sideways in prescribed U-channel.
4) Top capillaries should be *pushed into the top constraint*, and the top constraint not pulled out to the capillaries to ensure that no capillaries are too short, using the prescribed alignment push plate and 7.6 mm spacer plates. Top constraint should then be tightened down.

5) Using two persons, one should reach through the top of the array to pull the top constraint plate to the top, while another feeds the array through the bottom to prevent unnecessary bending and tension in the capillaries.
6) The bottom insert plate should be bolted in place while the second person manually holds the top constraint in place.
7) The top constraint should be un-tightened, and silicone should be checked so that it does not protrude past the bottom constraint plate. The U-plate and gasket on the thermal control chamber should then be slid into and around the top constraint plate.
8) The U-plate and top constraint can now be bolted to the thermal control chamber and U-plate, respectively. The constraint device itself should not be tightened at this point
9) The constraint device should be slowly tightened using a star pattern. Any excessive tightening of one screw too soon will cause the capillaries to skew in that direction, and misalign the capillaries to the buffer reservoirs.

The detection system for end-column fluorescence detection is described in Forest *et al.* [10] The detection system has been observed to perform as expected, allowing for detection of emerging fluorescent DNA to take place. A large focus of this thesis is to perfect the detection method, however these problems had little to do with the design of the detection system itself, but rather with the integration of DNA injection, buffer reservoirs, and lens arrays, which will be described in the 1st iteration results of this thesis. One critical item with the detection system is the requirement that all the instruments be at steady state to avoid drifting during experimental runs. In order to characterize the drift properties of the instruments, a cool-down trial was run where all instruments were run at their prescribed settings, and optical detection of the null capillary

array was performed. The LED excitement array requires a heat exchanger to maintain a constant 7 °C with an input into the LED array of 22 V @ 7 A. Additionally, the CCD camera requires a cool down period to reach a temperature of -10 °C, while pictures are being taken at 3 second intervals. Through this cool-down experiment, a number of required frames, and thus a required cool down time could be approximated. Below is a graph showing the upper and lower bounds of pixel counts for the CCD camera, illustrating the time to reach steady state.

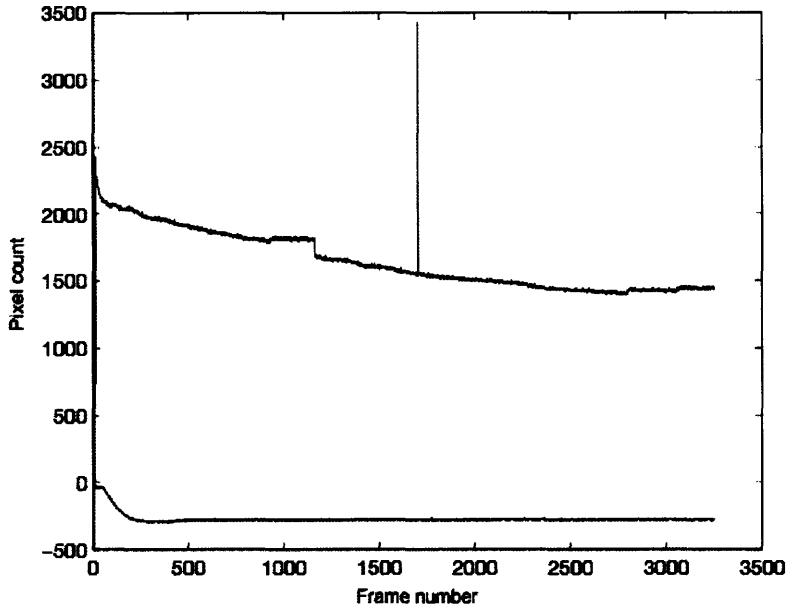

Figure 4: Cool-down run upper and lower bound pixel count.

As observed, there is required to be approximately 3000 frames taken to reach steady state, indicating a roughly 2.5 hour cool down period necessary before any experimentation is conducted.

Current research is being conducted regarding the integration of micro-forged injection molded lenslet arrays. A full description will be available within a Bachelors of Science degree currently being conducted by Miguel Saez in the MIT BioInstrumentation Lab, but which will be published concurrently with this thesis. The lenslet arrays allow the detection system to focus

primarily on the tips of the capillaries, enhancing the signal from the individual capillaries. The critical factors in consideration here are the alignment of the lenslet array to the capillaries, as well as proper focal length which will accurately focus on the end of each capillary. The integration of these requirements will be discussed during the first iteration designs of remaining required tools.

3.1.2 Remaining Required Tools

The remaining steps in order to run electrophoresis on the 100-channel array include the necessary tools to apply current and voltage across every capillary, introduce each end of the capillaries to a buffer fluid to maintain pH levels, and provide a safe method to integrate the DNA injection wells described in Forest *et al* [14]. With instruments designed to accomplish these steps, it will be possible to run CDCE on the entire 100 capillary array with ease.

4.0 Instrument Concepts

The critical component in design of the remaining necessary instruments is their ease of use by hand, and their integration into the procedural requirements of CDCE in a 100 capillary array. In order to accomplish the remaining required tasks, it was determined that three separate devices needed to be constructed to accomplish electrical conductivity, optical detection viewing, buffer fluid contact, and DNA injection. A buffer reservoir will allow the capillaries to come in contact with a reservoir of buffer solution which will be able to accomplish both electrical conductivity to all 100 capillaries, as well as exposing the tips to a fluid pH buffer which will not only maintain pH stability during electrophoresis, but prevent the injected polyacrylamide gel from evaporation. Two of these instruments are needed, one at both ends of

the capillary array. DNA injection may be accomplished by the integration of the existing 100-microwell plate to a device which will allow precise alignment of the wells to the bottom of the capillary array with minimal chance of damage or misalignment. Both this device and the buffer reservoirs will require a simple, hand operated method of alignment to the capillary array in order to facilitate quick interfacing and minimal risk of damage.

4.1 Buffer Reservoir Design

The concept of the buffer reservoirs was constructer off of previous work with introducing up to 5000 capillaries into a buffer reservoir. However, this device proved to be extremely leaky, with difficult assembly techniques and a lack of self-alignment, which required each capillary to be inserted manually. This device was never proven to work with ease in a 5000 capillary array, but served to provide much of the basis to design the next iteration of the device.

The device requires that it can be inserted to the capillary array in less than 10 seconds to prevent contamination and/or evaporation of the gel matrix, and to seal upon insertion to prevent leaking of the buffer fluid. Additionally, the capillaries must align themselves to within 50 μm radially to ensure optical detection. It also must be able to survive a high applied voltage (10 kV) and a chemically corrosive environment.

The initial consideration in designing the device was to first develop a method to allow the capillaries to align to a respective ports with minimal action from the user. It was devised that a coarse alignment may be accomplished through the use of two 6mm steel guide pins inserted into the thermal constraint device. The remaining alignment could then be accomplished through the use of conical tapers to guide each capillary tip into a 400 μm hole. The device concept is illustrated below in Figure 5.

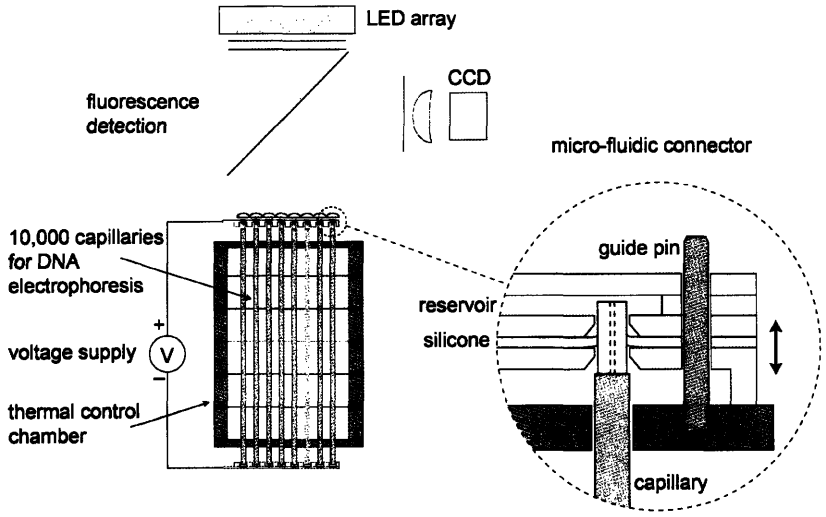

Figure 5: Instrument concept. Alignment is accomplished using the pink colored guide pins, while the yellow capillaries are guided into their ports by a conical tapered hole. Modified from [1].

In order to predict repeatability and accuracy of insertion for the capillaries into a connection interface, a system error budget [15] was created. With the capillary tip as the "tool," and the fluid connection port as the "workpiece," we proceeded to trace random errors through the structural loop to predict the maximum mechanical alignment error. Random errors were tallied from the capillary tip to a guide pin interface to conical entry ports through eight coordinate systems. These errors were dominated by machining tolerances and capillary radial misalignment. Random error results are displayed in Figure 6; systematic errors were negligible, as were axial (z) errors. The detailed analysis is shown in Appendix B.

	Random errors (mm)	Root-Sum-Squared random errors (RSS) (mm)	Average of random & RSS (mm)
Δx, Δy	0.38	0.21	0.30

Figure 6: Error budget for capillary alignment structural loop

Thus the predicted maximum alignment error between the capillary tips and the conical fluidic ports is 0.30 mm. We therefore designed the entry port for each capillary to have a radius large enough to tolerate this misalignment; 0.5 mm radius entry ports can tolerate a misalignment of 0.32 mm. The connector is translated along the guide pins, causing each capillary tip to be directed by a pair of conical tapers (primary and secondary) into a 400 μm hole. These conical ports independently and passively bend the capillaries into an aligned grid with 20 μm radial accuracy, spaced 1 mm apart. The top buffer reservoir device is illustrated below in Figure 6 in an exploded view.

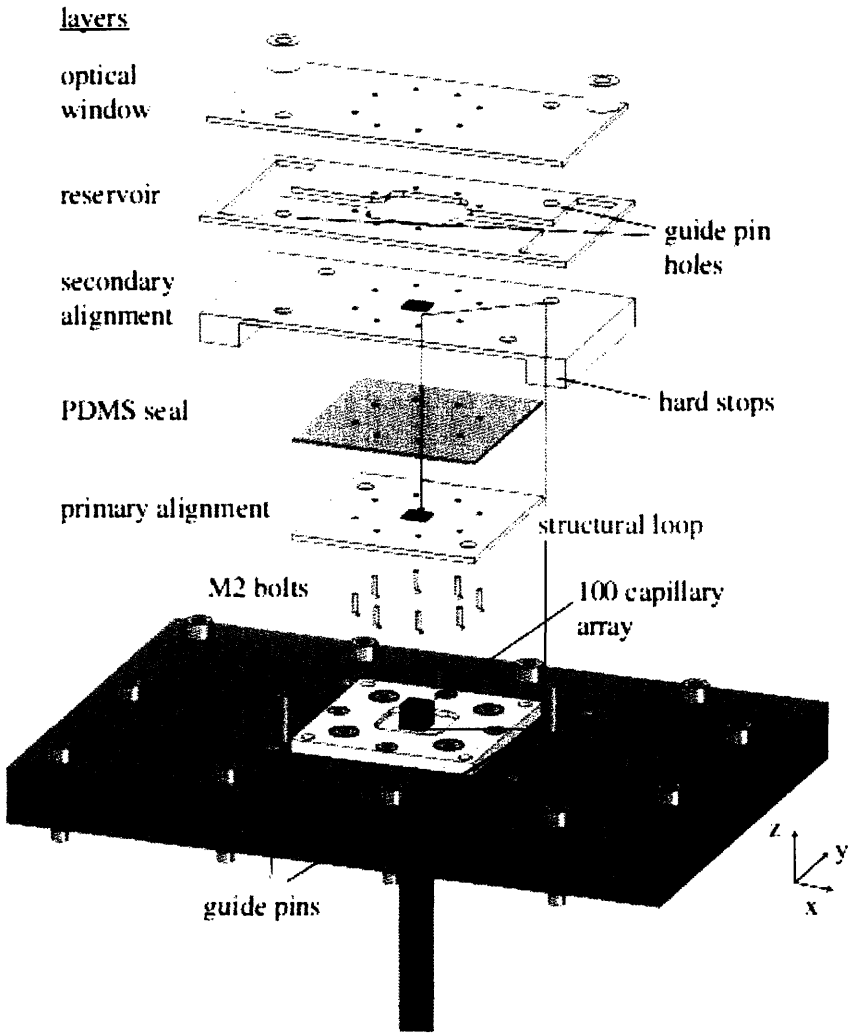

Figure 7: Exploded model of the top buffer reservoir.

As shown, entry ports on the primary alignment layer are registered to those on the secondary alignment layer. This secondary alignment layer has reamed guide pin holes which are machined in the same setup as the conical ports for accurate registration. After the guide pins provide coarse capillary alignment, the primary and secondary alignment layers engage the capillaries.

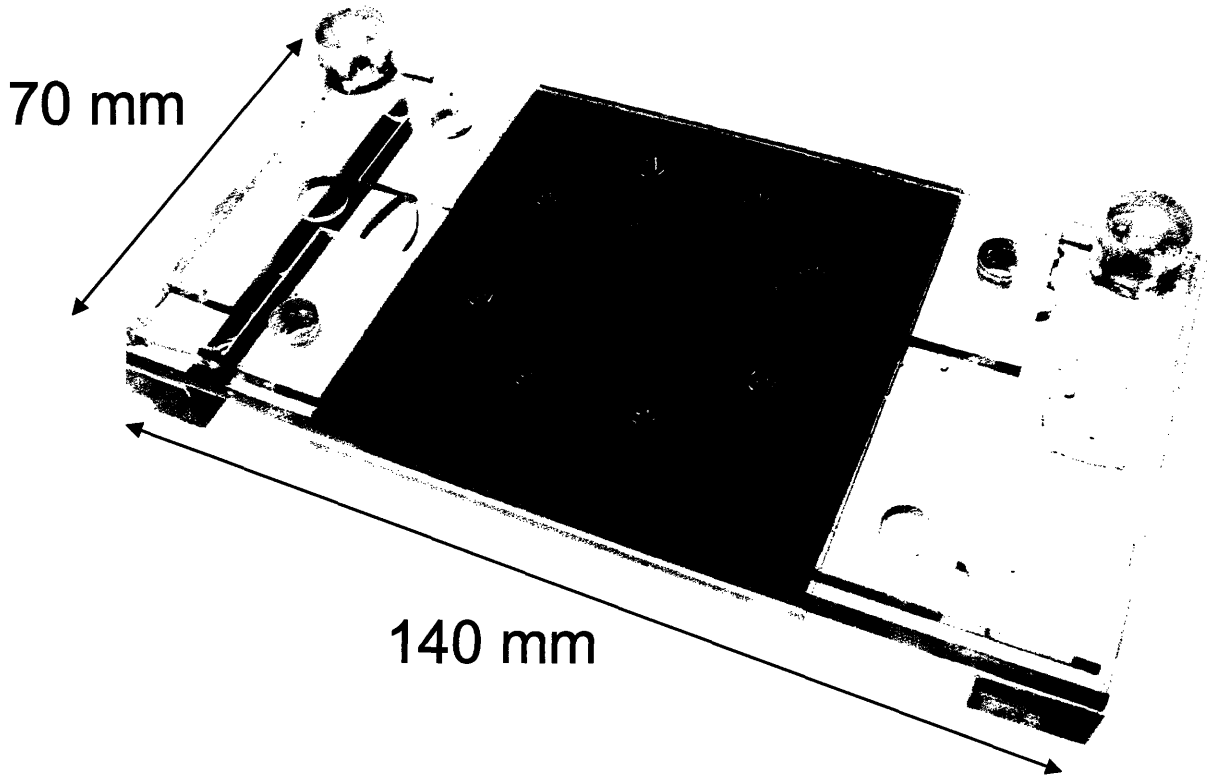

Figure 8: The completed top buffer reservoir.

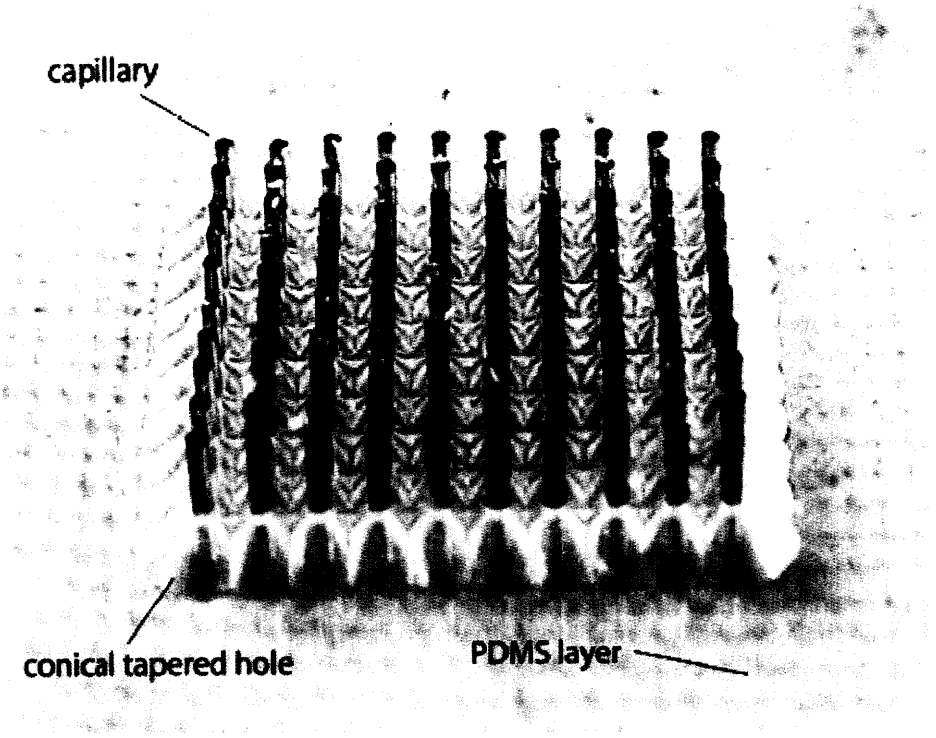

Figure 9: Photo of 100 capillaries (OD 360 μm) inserted and sealed in the buffer reservoir.

The entire device is constructed using four separate layers of 1.8 mm thick polymethyl methacrylate (PMMA), fluidically sealed with a layer of poly-(dimethyl siloxane) (PDMS) and bonded with PMMA solvent methylene dichloride. Each PMMA layer is laser cut (Trotec Speedy 100) and the conical ports are center drilled in a Haas VF-OE milling center with 381 μm center drill (trade size 0000) at 21,000 rpm, followed by a through hole using a 400 μm drill bit at 25,00 rpm.

As the capillaries are inserted into the device, they pass through the PDMS layer, which and seals around their perimeters. When the capillaries are removed, the silicone reseals, preventing escape of fluid from the reservoir.

Translation along the guide pins is limited by hard stops on the secondary alignment layer, preventing capillary damage. During electrophoretic separation of DNA within the capillaries, a 5 mL buffer solution in the reservoir layer permits application of high voltage (up

to 10 kV tested) to the capillaries via a platinum wire electrode, as well as collection of the eluted DNA. Detection of DNA is permitted by a PMMA optical window layer. (Figure 9 photograph taken through this window).

The use of these coarse guide pins has also been incorporated into the design of the lenslet arrays, which are being concurrently developed with these buffer reservoirs. Alignment is achieved in the same fashion as the buffer reservoirs are to the capillary array, by the remainder of the guide pins which extend beyond the top of the upper buffer reservoir. Thus it is possible to achieve repeatable, accurate alignment in the x-y direction with the guide pins. Focal length was calculated to allow the lens array to be placed directly on top of the buffer reservoir, and focus on the end of the capillary array. Thus, the lens array simply needs to be pushed as far onto the buffer reservoir as possible, and, it will focus on the proper z-coordinate location.

4.2 Buffer Reservoir Design Verification

4.2.1 Capillary radial alignment accuracy

For each of the capillaries shown in Fig. 3, we measured the capillary tip alignment before and after insertion into the 100 port connector. For the 100 capillaries tips protruding 8 mm from an elastomer constraint device [8], the 3σ radial deviation from a regular grid with 1 mm pitch is 187±7 μm. Since the holes in the fluidic ports are only 400 μm in diameter, the 360 μm diameter capillaries must be aligned to, at worst, 20 μm radially after insertion.

4.2.2 Repeatability

The repeatability of insertion was measured by a 100 trial experiment. The micro-fluidic connector was inserted to the 100 capillary array 100 times, resulting in a total of 10,000

individual capillary insertions. During the course of these trials, 6 capillaries were rendered unusable. In total, 9517 out of 10,000 capillaries were successfully inserted, for a 95.2% total insertion success. Repeatability data is shown below in figure 10:

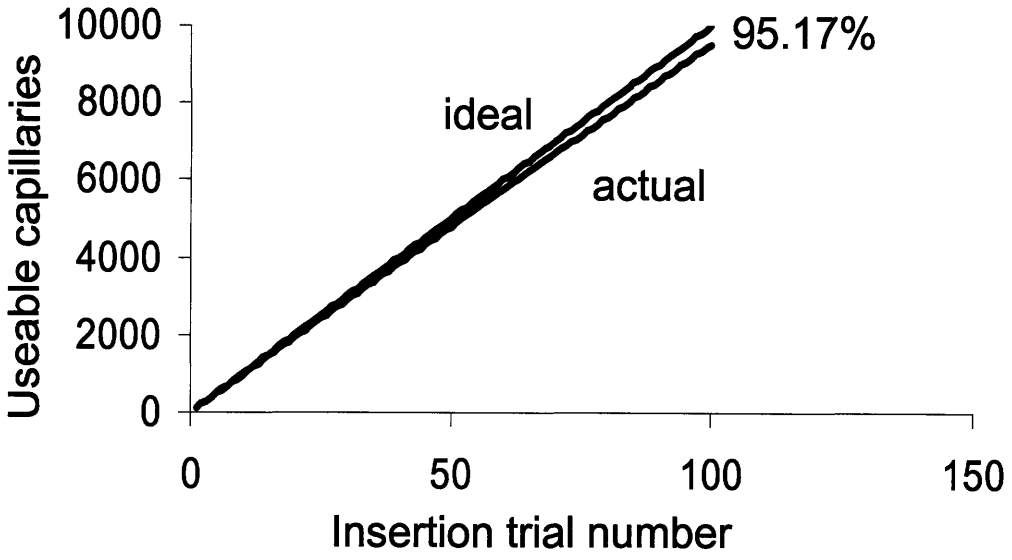

Figure 10: Repeatability data for 10,000 insertions versus ideal capillary usage.

4.2.3 Electrical and fluidic connectivity

A test to verify electrical and fluidic connectivity was conducted. During electrophoretic operation, the capillaries, filled with a polymer matrix, are inserted into micro-fluidic connectors at either end. In this experiment, we inserted the ends of a single, gel-filled capillary into two connectors containing buffer solution. Platinum electrodes were used to apply a 4 kV potential difference between the ends. A current of 8 μA was measured indicating electrical and fluidic connectivity.

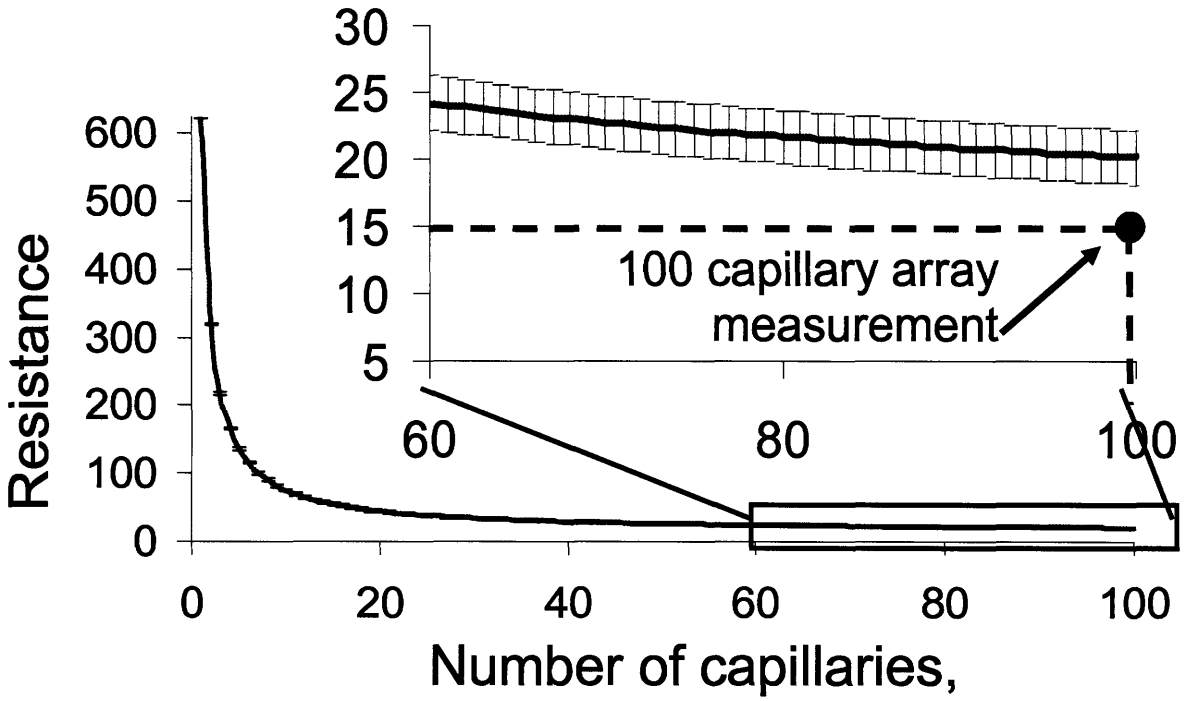

Figure 11: Electrical resistance measurement (red dot) for the 100 capillary array.

Figure 10 allows for determination of the number of capillaries (n) filled with polyacrylamide gel, as well as showing electrical and fluidic connectivity to those n number of capillaries. Total system resistance was measured as 19 MΩ.

4.3 DNA Injection Interface

The final component in achieving DNA electrophoresis is a method to introduce the DNA micro-well array to the bottom of the capillary array. Previous work describing the construction of a silicon-based DNA microwell array is outlined in Forest *et al* [14]. The device used in DNA electrokinetic injection is the silicon device, machined via sink EDM (Charmilles technologies, Roboform 30), using a plunger manufactured in a wire EDM (Charmilles Technologies Robofil 1020SI). The silicon wafer is then anodically bonded to a borosilicate

wafer and PDMS sealed. Once complete, the wafer was machined to a 50 mm × 50 mm square to be mounted in device which will allow it to interface to the capillary array.

The device to be constructed to allow interfacing to the array is the remaining tool necessary, and is easily modeled after the buffer reservoir passive alignment technology. The primary requirement is that the micro-well plate is accurately registered to the existing guide pins that coarsely align the buffer reservoirs. By using the same pins in combination with tapered conical guide holes, the individual capillaries can each be guided to their appropriate corresponding microwell for DNA injection.

A layered PMMA device was utilized to contain the silicon micro-well array. A bottom plate where the micro-well array would mount was machined in a Haas VF-OE milling center with an appropriate pocket, and required guide pin holes to initially register the device. A top layer is used to seal the micro-well array, and to incorporate the conical guide hole array which is manufactured in the similar way as described in Section 4.1 describing buffer reservoir design. In addition, a notch was cut into both PMMA plates to allow an electrical connection to the microwell array to achieve electrical conductivity for electrokinetic injection. The micro-well array was registered to the guide pins by using individual capillaries to register the four corners of the array to a proper position within the pocketed plate. By using individual 6mm guide pins to align the conical guide plate and pocket plate, the silicon array could be placed in its appropriate position and secured with hot glue. The top plate is then removed and the silicon micro-well is again hot glued around its perimeter. A photo of the completed device is shown below in Figure 12.

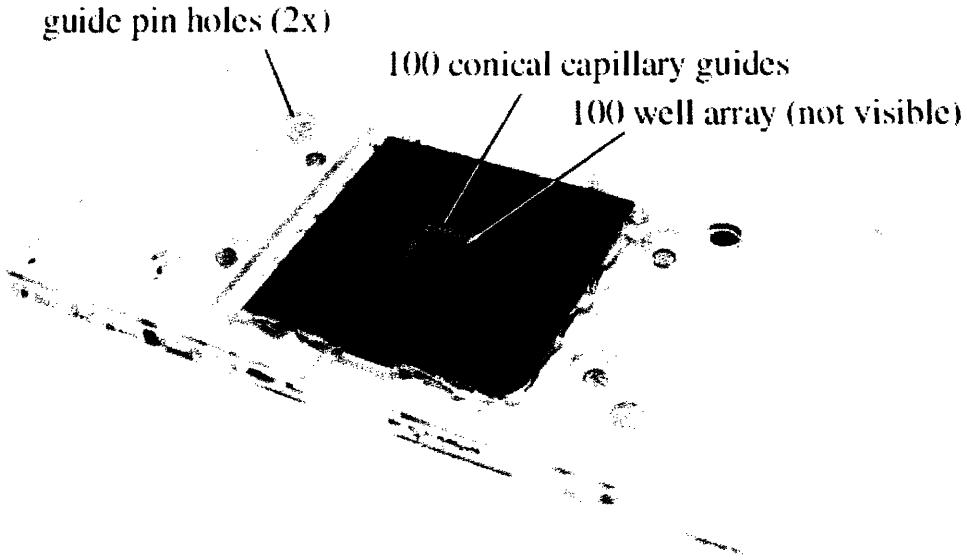

Figure 12: DNA injection device with incorporated micro-well array.

4.3 DNA Injection Design Verification

Verification of the device will primarily be shown in the successful detection of DNA primers in injection. It can be said that the device performed as required to load DNA primers into the 100 capillary array, but the results will be discussed in more detail in both 1st and 2nd iteration results. At this point, only procedural verification of the device can be described.

The array successfully accepted injection of 20-base primer fluorescently labeled with Alex-aFluor 488 Synthegen at 20 nM concentration. 300 nL of solution was successfully injected into multiple capillary arrangements, including single capillaries, x-pattern, and alternating wells. The device is easily operated, with injection taking place without the conical guide plate in place. Once the desired wells are loaded with primers, the top plate is registered to the microwell array by placing two free 6 mm guide pins in the holes used for coarse alignment, followed by the top plate being placed above the micro-well array. The top plate is then secured and the free 6 mm pins are removed, and proper electrical connection is made. The plate was successfully mated to the guide pins, achieving electrokinetic injection at 1 μA, 2 μA, and 10 μA per capillary.

5.0 First iteration of procedures

A main concern in the development of the UTMS device is the procedural requirements needed to successfully conduct CDCE on a large scale. It is as equally important as the design of individual mechanical, thermal, electrical and optical subsystems in the device, and has required multiple iterations to define a set of procedures which will prevent any of the problems encountered during the experimental runs of this thesis. Outlined below will be a list of all procedures necessary to run a 100-capillary array in CDCE, with descriptions and background of certain steps as necessary.

1) All instruments which require cool-down time must be set to run 3 hours prior to electrophoresis run to prevent drift. Refer to Section 3.1.1 for detailed reasons. Instruments required to be activated include: LED power supply (HP 6653A DC power supply) at 22 V and 7A, LED array heat exchanger (VWR Recirculator) at 7 °C, CCD Camera (Apogee, U10) cooler set to -10 °C and Maxim DL camera imaging software (Maxim DL v. 3.2.1, Sehgal Corp) set to take pictures every 3 seconds, as will be done in CDCE imaging run. All these devices should be activated to the state they will be in during CDCE.
2) Capillaries should be checked for clear flow. If the array has been disassembled, all capillaries should be checked in the single-capillary pressure loader with capillary wash solution to check for any obstructions which would prevent gel loading. In some cases, more than half of the 100 capillary array has been rendered unusable because of clogging by some unknown factor. An assurance against this is to either keep the array assembled

and protect it within the UTMS, or check capillaries before insertion into the constraint device. Gel loader should be used at 275 kPa (40 Psi) in conjunction with Burkert Solonoid to easily control pressure within reach of the user via a toggle switch. Solonoid is powered using Kepko power supply (MPS 620M). A photograph showing the single capillary setup is shown below:

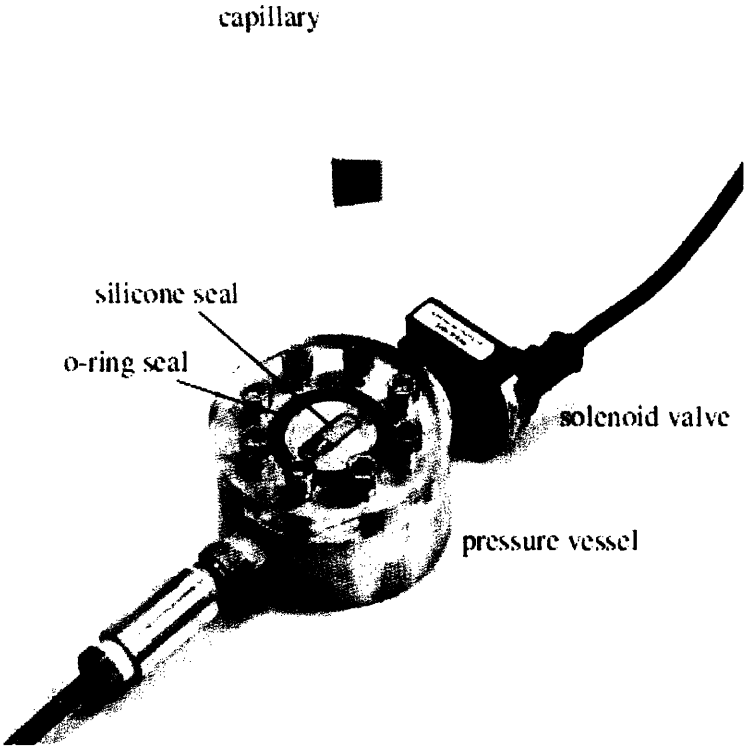

Figure 13: Single capillary flow check using single capillary gel injector and capillary wash solution. Taken from [12].

3) Capillary array should be assembled as described in Section 3.1.1. The critical steps in these procedures are: to ensure marked corners are in alignment to ensure separate coordinate systems are aligned to meet requirements of system error budget, two persons are used to minimize risk of damage to the array, and that the upper constraint plate is loosened prior to u-plate insertion.

4) All alignment should be checked with buffer reservoirs. Because edge effects are negligible in the lower constraint device, primary attention should be paid to the top capillary constraint. The top buffer reservoir should slide on easily to a point where no sounds of cracking are heard, and there is no strong resistance to mating the reservoir to the capillary array. Ideally, the buffer reservoir should be able to sit on the top of the capillary array with very little force, with all capillaries registered to the initial alignment plate and resting just below the PDMS sealing layer. If this alignment is not achieved, the re-tightening of the top capillary constraint should be redone. If this does not solve the problem, the entire array must be disassembled and the top capillary constraint device should be checked for alignment between the separate plates and intermediate silicone layers. An adequate method observing alignment is to observe the 100 hole array against a lighted background. If light can be observed through all 100 holes, the respective sections are aligned. This procedure should be repeated until all layers are incorporated, and then secured using tightening bolts.
5) The capillary array should be washed before any gel injection. This should take place regardless of whether or not the array was evacuated of gel during a previous experiment, in order to free any particles which may have contaminated the array during down time. Gel wash solution may be loaded into the gel injection device, and mounted and sealed to the bottom of the thermal control chamber and lower constraint device using the incorporated 4 bolts. Capillary wash should be injected at 275 kPa (40 Psi) for 10 seconds using the solenoid and power supply as outlined in step 2. Initial development of the capillary wash procedure is outlined in Appendix A of Nathan B. Ball's MIT Bachelors of Science Thesis [12]. Solution should emerge from the top of the capillary array

extremely quickly if there is no gel in the system. If there is previous gel in the system, the buffer wash solution will be visible as a much more rapidly emerging and less viscous substance. Care should be taken to rinse the expelled gel from the top constraint device to maintain a clean instrument

6) Gel Injection can now take place. Using the instruments developed in Nathan Ball's Thesis [12], gel can be injected by loading the instrument well with polyacrylamide gel, and mounted to the same position as described in step 5. Gel should be injected using the combined solenoid and power supply mentioned in step 2, at 275 kPa (40 Psi) for 1 minute. In order to determine if gel is emerging from the top of the capillary array, rather than wash solution, the top of the array can be dabbed with a kimwipe cloth. If the fluid is easily absorbed, with no residue, the fluid is still capillary wash. However, if the fluid creates long, thin strings when pulled away, the fluid is gel. The entire array can be checked by wiping the top clean of buildup using a kimwipe, and observing the tips using a 10x handheld lens. If small bulbs form on the top of each capillary without falling down the side, gel is the emerging solution. Shown below illustrating the gel loader mounting position for capillary washing and gel injection

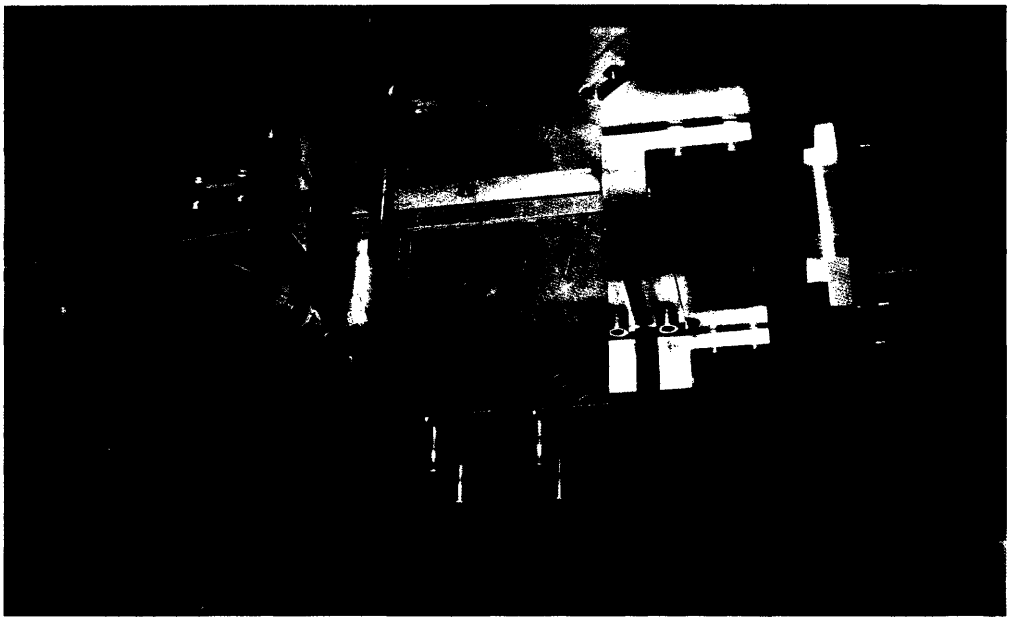

Figure 14: Gel / Capillary wash pressure injection device mounted to the capillary constraint device.

7) The buffer reservoirs can now be inserted onto either end of the array. The first device to be inserted should be the top buffer reservoir, as it can be used to clean off the remaining gel bulbs on the tips of the capillaries as it is pressed into position. The initial alignment should be accurate if step 4 is followed to remove any procedural misalignment. The top buffer reservoir can be pressed on until it comes in contact with the constraint device. The gel injector can now be removed, but the capillary array must be washed before any buffer reservoir is placed on the array. This is simply accomplished by spraying a jet of Millipore water onto the protruding capillaries to rinse them. Once all gel is adequately removed, they can be dried. Drying is an extremely important step, as it will prevent the cross-contamination of DNA on the microwell plate during DNA injection. Once the capillaries are dried, the lower buffer reservoir must be placed on within the 10 s time limit. The bottom reservoir can then be secured using the attached quick pins to prevent

gravity from slowly drawing the reservoir off the capillary array. Shown below are photograph illustrating the top and bottom buffer reservoirs in their final positions.

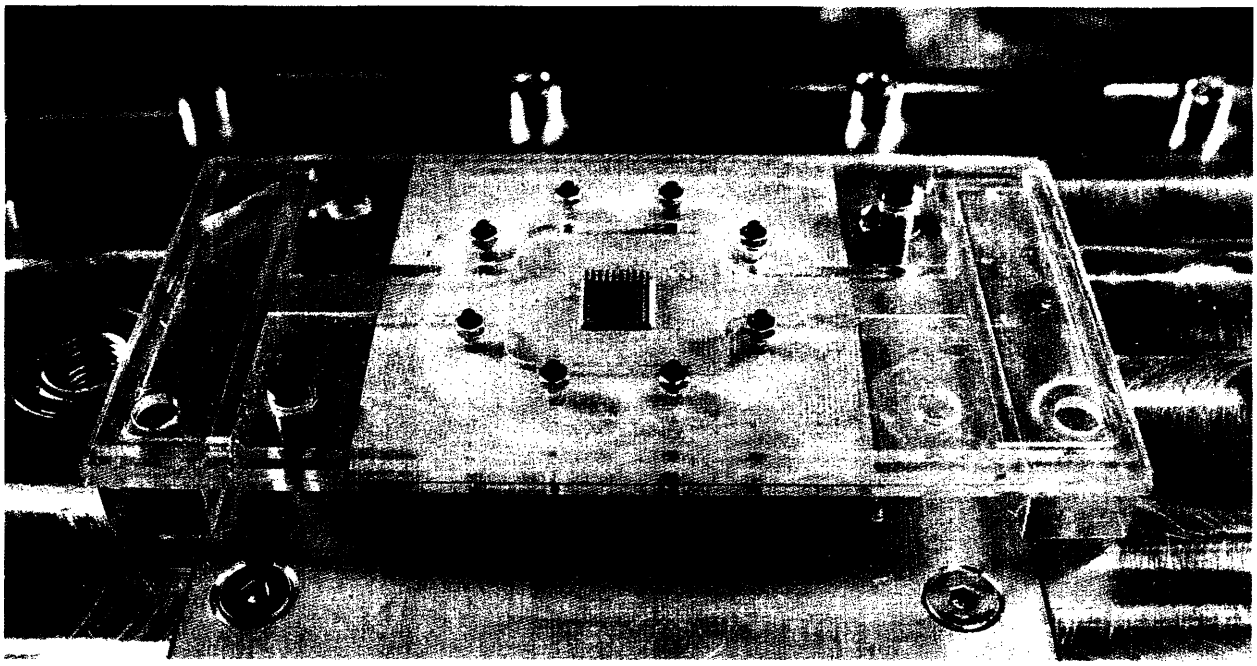

Figure 15: Top Buffer Reservoir interfaced with the capillary array.

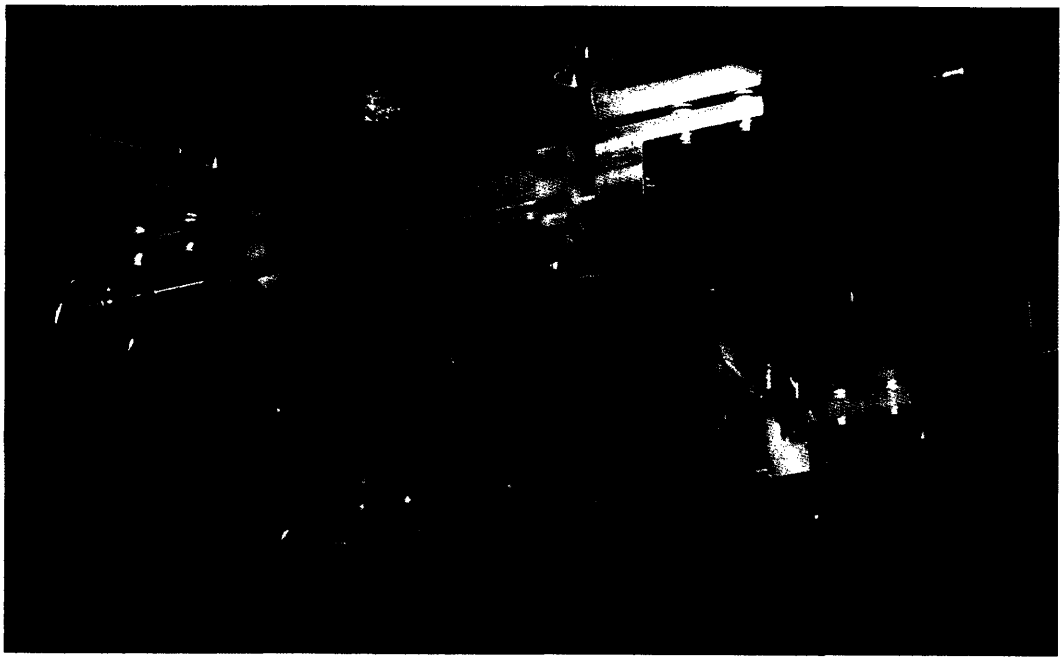

Figure 16: Bottom Buffer Reservoir interfaced with the capillary array and constrained with quick pins.

8) DNA injection can now be conducted. This is the critical timing point within this procedure. Once this step has begun, the run must be completed or entirely aborted because of the nature of the DNA. Excessive time spent in the DNA micro-well plate can lead to evaporation of the solution, as well as excessive time after DNA injection the DNA can diffuse back into the buffer solution. The first step is to connect the power supply (Spellman CZE1000R DC Power Supply) to verify injection loading conditions are met. 100 capillary array experiments are run at 100 μA, or 1 μA per capillary for 30 seconds. Additionally, the injection plate must itself be prepared before DNA can be loaded onto the plate. In order to minimize time after DNA loading, guide pins should be placed in the proper holes, and necessary tightening bolts, tools, and top alignment plate should be kept in close proximity. Leads to the power supply should be attached to the cathode on the top buffer reservoir, and to the silicon plate. 300 nL of 20-base primer fluorescently labeled with Alex-aFluor 488 Synthegen at 20 nM can now be injected into each required micro-well. Once injected, the top plate can be placed on the micro-well array and secured with tightening bolts. The array can the be loaded by hand to the coarse alignment pins, and pushed up to the capillary array. There should be a sufficient amount of resistance met when the capillaries reach the bottom of the silicon micro-well plate. At this time, the power supply can be activated for 30 seconds and the required 100 μA. Once completed, the DNA injection well can be removed and replaced with the lower buffer reservoir

9) The array is now ready for CDCE. The lenslet array can be mounted above the buffer reservoirs by being pushed down to the buffer reservoir, and the array can be pushed from the loading position to the detection position on the guide rails sealed with a black

cloth to prevent ambient light from entering the detection chamber. The camera should then be reset to a new folder directory, and pictures should begin from the number 1. Immediately after this, the power supply can be activated at 100 μA for 2 hours, in order to ensure the DNA primers migrate completely across the capillary and emerge on the opposite side.

6.0 First iteration results

The test decided on to run in the 100-capillary array was the replication of the MIT logo through selecting corresponding microwells to create each letter as they emerge from the capillary array. This arrangement would be able to test the new instruments in being able to verify optical detection of primers, as well as successful injection of primers with the new DNA micro-well housing. Shown below is the raw data as shown after image processing.

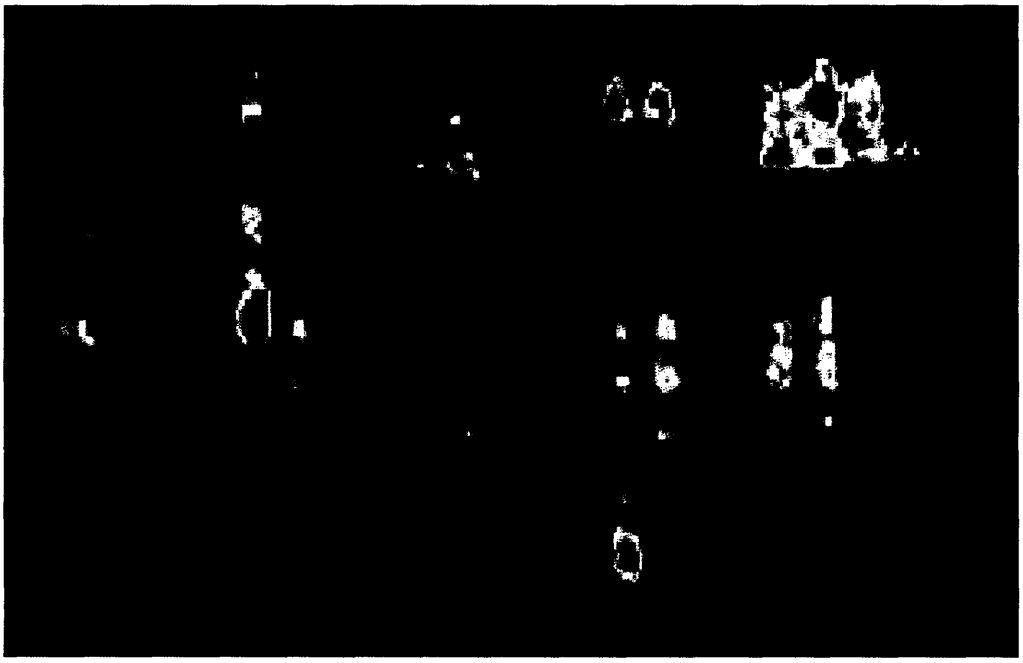

Figure 17: MIT Logo as raw data observed through UTMS detection system.

As can be observed, the DNA injection was successful and the buffer reservoirs allowed optical detection of the emerging peaks through the detection window at the top of the reservoir. Each of the letters observed in Figure 17 are separate trial runs, and edited in Adobe® Photoshop to bring them into the MIT logo layout.

The image analysis software used to create this image operates by scaling the raw pixel value count, which corresponds to the number of photons impacting each pixel, into a color map, and subtracting the initial image in the sequence to only display changes in pixel count from the initial frame. By using this method, any initial noise in the system can be removed without any effect on the detection. Initially, the program used to conduct this image analysis was rather complicated, creating a massive three dimensional matrix which would hold all pixel values of every picture taken during the run, scale it manually by setting the lowest pixel value to 0 and the highest to 1, and then scaling to a 256 color map, and inserting the pictures to a movie. This program would cause even the quickest computers in the Bioinstrumentation Lab to freeze, necessitating the creation of a simpler code. This new code utilizes the function *imagesc*, which can automatically scale a picture to a given color map. The massive matrix used to create a movie still remains, but the procedures done to each individual picture are now simpler, and can be run quickly on less sophisticated computers. The derived MATLAB code is shown in Appendix C.

The main issue observed in this experiment is the problem of crosstalk. Observe the letter "M" between the first two columns of capillaries, and below the cross of the "T". There is illumination in locations where there was no DNA injected, and there is no discernable pattern as to where the stray DNA primers may be heading towards. These can easily be seen as caused by the capillaries nearest too them, but the issue remains what factor has caused these unloaded

capillaries to show as if there has been DNA loaded into them. If the array is to be loaded using all 100 capillaries, this sort of crosstalk is unacceptable and would result in incorrect reading across the board, giving false pixel counts for many of the capillaries. It is an issue which will be addressed in the second iteration of the buffer reservoir design.

7.0 Second design iterations

There are many observed faults with the initial development of the buffer reservoir and DNA injection plate. Primarily is the issue of crosstalk across the capillary array during end column detection. Each signal must be isolated from its neighbors and not influence a nearby optical reading in any way.

Additionally, the buffer reservoirs are themselves are over constrained, and require a large amount of force because of the friction occurring between the coarse alignment steel guide pins, and the PMMA layers. It is this difficult to determine if there is any damage being done to the capillary array during insertion, and the large amount of force being applied by hand increases the chance that the entire array may be damaged in the event of a slip.

Electrical conductivity has also become an issue. It was discovered early on before the MIT logo experiment was conducted that there was a closed circuit not only through the capillaries, but through the thermal control chamber through the alignment pins. A quick fix was to replace a layer of the thermal control chamber with multiple layers of laser cut PMMA, but this would only be a temporary solution, the chamber now would no longer seal. An alteration is necessary somewhere in the system to fully isolate the top buffer reservoir from the bottom constraint plate in order to fully direct the current through the capillary array.

7.1 Buffer Reservoir – Second iteration

A hypothesis was formed that the reason crosstalk was occurring near injected capillaries was caused by the migration of DNA along the detection plane of the optical detection system once it had exited the capillary array. While the DNA fragments move much quicker within the buffer solution, there is still a substantial amount of time when the primer segments can be picked up by the optical detection system. It was thus decided to move the detection plane above that of the fluid reservoir layer in the upper buffer reservoir assembly in order to allow the DNA fragments to move below the detection plane once they had exited the capillary. The detection plane would thus be focused on only the tips of the capillaries, which would no longer lie in the same plane as the majority of the fluid reservoir. This separation of planes would be accomplished by micro-milling an individual pocket in the optical window of the buffer reservoir to both isolate the tip from its neighbors, as well as allow each tip to be raised above the plane of the fluid reservoir layer. A diagram of the new layout is shown below in Figure 18.

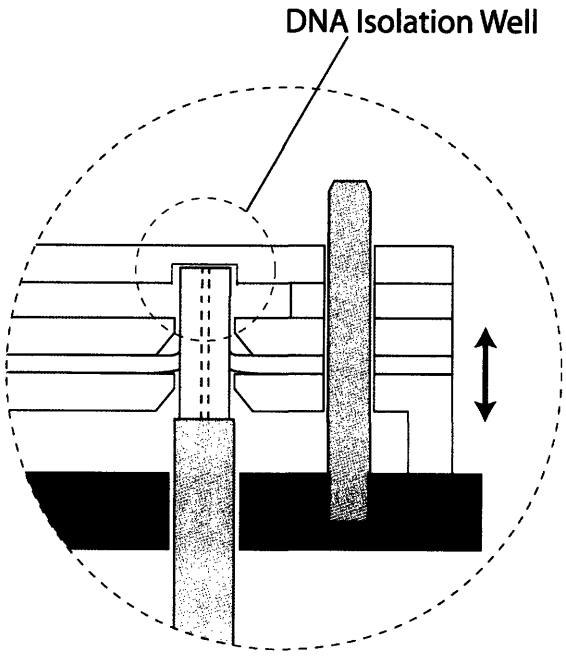

Figure 18: Diagram of new upper buffer reservoir with pockets to isolate capillary tips.

The micro milling procedure done to create a 10 × 10 array of pockets creates an opaque bottom, which would inhibit optical detection by the CCD camera. It was thus necessary to apply an Dichloromethane treatment to the pockets in order to restore clarity. This procedure is accomplished by bringing a small volume of dichloromethane to boiling in order to create dichloromethane vapors. The intended sample is then placed above the boiling liquid to expose it to the vapors. This process causes tool marks and other surface marks to become transparent, but care must be taken to not melt the surface to the point of severe deformation. After multiple test pieces, it was determined that the best procedure was to expose the intended surface in multiple short, 5-7 second intervals. The optical window layer was milled and exposed to the dichloromethane treatment for a total of 30 six second intervals. Shown below in Figure 19 is the before and after photographs of tool marks and cleared surface, and the complete inserted array into the capillary pockets in Figure 20.

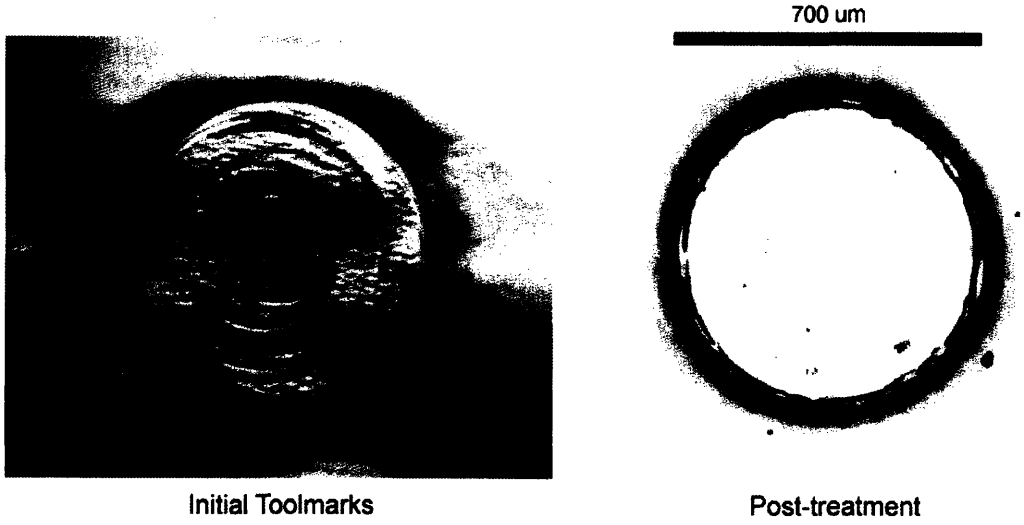

Figure 19: Dichloromethane treatment, before and after photographs of capillary isolation pockets.

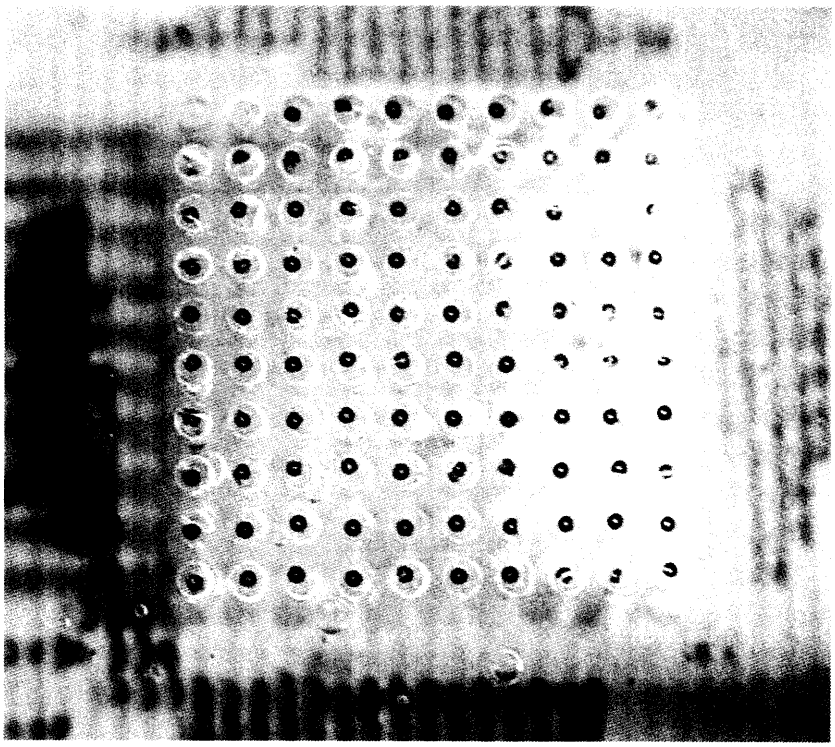

Figure 20: Capillary array inserted into new buffer reservoir with tips in isolation wells.

In the first iteration of design, the top buffer reservoir was assembled using methylene dichloride to join each of the layers together. Thus, once the top optical window plate was glued in place, it would be impossible to remove. It was decided that this second iteration should allow for modifications to this plate, if necessary, without calling for construction of a completely new buffer reservoir. The top plate of the buffer reservoir is now sealed using a PDMS layer identical to the sealing layer used in the same buffer reservoir, but laser cut (Trotec Speedy 100) to the same pattern of the fluid reservoir layer. A bolt circle around the buffer reservoir ensures that the top layer seals firmly to prevent leakage and evaporation of the fluid. A photo of the completed buffer reservoir is shown in Figure 21.

The over constraint of the buffer reservoir was addressed by modifying the alignment ports on the buffer reservoir rather than attempt to modify the existing guide pins on the thermal control unit. A hole and groove design was used to replace the double-hole design which over

constrained the buffer reservoir in the x and y directions. A hole and groove will only over constrain the y direction, but relieve over constraint in the x direction while still preventing rotation. Experimentation on the array prior to CDCE runs has shown that the new buffer reservoir requires significantly less force to mate to the capillary array, and it is now possible to notice a resistance force is the capillary array is misaligned, rather than misinterpreting said force to be a result of friction between the buffer reservoir and guide pins. The final buffer reservoir with pin and slot is shown in Figure 21.

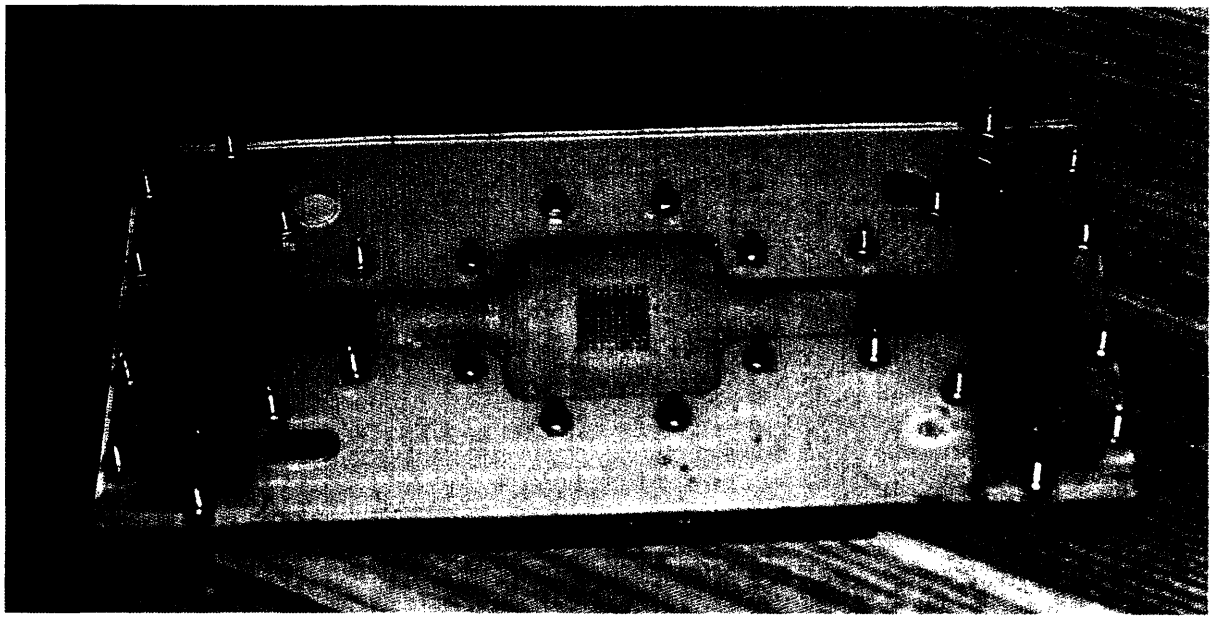

Figure 21: Competed second iteration of the top buffer reservoir.

In order to address the open circuit caused by electrical conductivity through the guide pins, it was necessary to derive an alternative to the quick fix of replacing a layer of the thermal control chamber with acrylic layers. The path chosen was to attempt to accept that pure isolation of the buffer reservoir from the guide pins would require a prohibitive amount of time, but rather to attempt to isolate the entire top buffer reservoir as well as the guide pins and constraint device from the rest of the thermal control unit. There would thus need to be impedance to electrical

flow both through the water that would eventually fill the chamber, as well as through the structure of the thermal control chamber itself. These two goals could be achieved through two separate methods acting in conjunction

The water level in the thermal control chamber has been seen to not reach the absolute top of the control chamber, and can be somewhat controlled by the flow rate into the chamber. [16] Additionally, the required heated length of the capillaries was below the total length exposed in the thermal chamber, indicating that the water level did not need to be at its maximum to provide adequate heating to denature the DNA. Thus, by lowering the water level below where it would come in contact with the top of the chamber and metallic constraint devices, electrical conductivity through this path could be avoided.

Additionally, to avoid an open circuit through structure of the chamber, the top plate of the thermal chamber was re-machined in a CNC milling center (Haas VF-OE) out of delrin, which would prevent electrical conduction through the plate to either the aluminum structure modules or to the water. Thus, rather than only the buffer fluid being maintained at electric potential, the entire buffer reservoir along with constraint plate is now at the required potential to run CDCE. A photograph of the re-machined top plate is shown below in Figure 22.

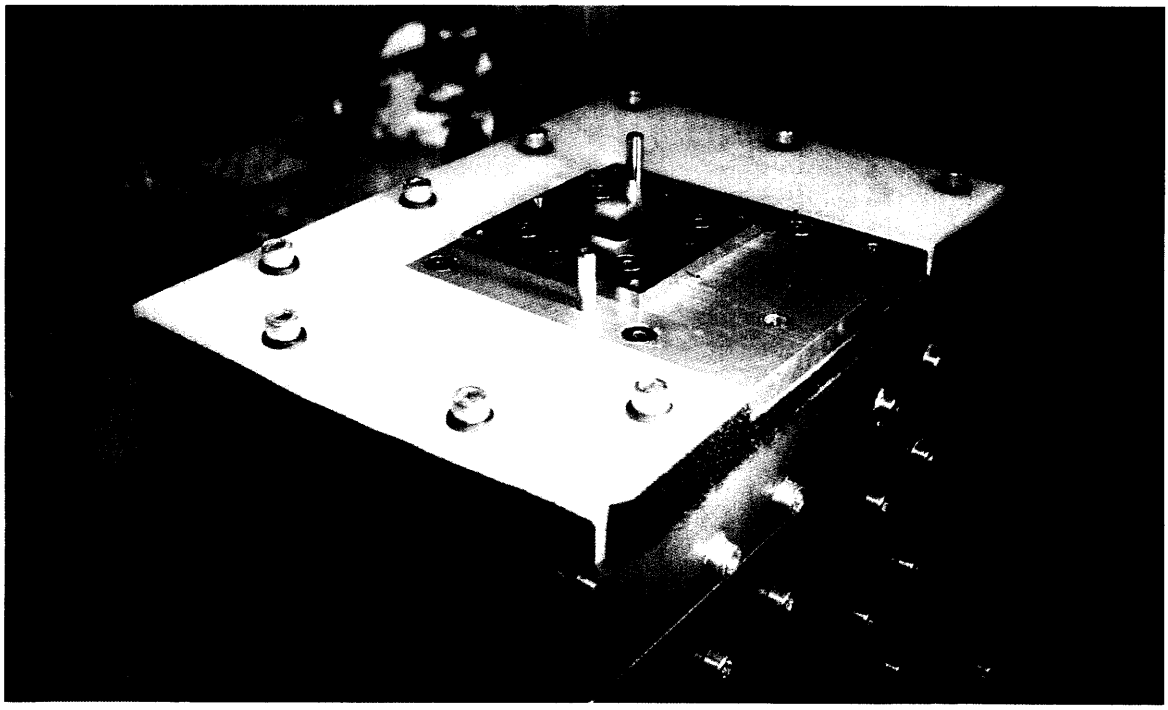

Figure 22: Delrin top plate of thermal control unit, with assembled constraint device and capillary array.

8.0 Second Iteration Procedural Changes

The integration of pockets into the buffer reservoir created an unexpected problem when filling the fluid chamber with buffer solution. It was observed that the pockets themselves would not fill with fluid, but rather an air bubble would remain within the pocket. Multiple different approaches were taken to remove these bubbles before use in CDCE by altering filling methods and also subjecting the reservoir to vacuum. However, neither of these procedures succeeded in evacuating the air from the isolation pockets.

It was discovered that a simple solution existed with the current instruments used in running the UTMS. By using the gel pressure loader in the same fashion that is used to wash the capillaries, buffer solution could be loaded into the well to inject into these pockets if the buffer reservoir were mated to the top of the capillary array. This successfully would remove the air from the isolation pockets, and make is as simple as to shake out the air by hand. Listed below is

a procedure to remove the air from these pockets which should be inserted between steps 5 and 6 as outlined in Section 5.0 regarding first iteration procedures.

5.1) Following washing, the buffer reservoirs should be inserted onto the capillary array to prepare for buffer solution injection to remove air pockets. The gel loader can be removed and cleaned, and buffer solution loaded into the well, and reattached as in step 5. Buffer solution can now be injected at 140 kPa (20 Psi) for 5 seconds. Care must be taken to not use all of the buffer solution and then inject air into these pockets. The gel loader need only be run for an extremely short period of time. This procedure will cause the bubbles to be pushed out of the pockets, which can then be evacuated by removing the buffer reservoir and shaking the bubbles out. The procedure should be repeated once again to ensure complete removal of air, and the buffer reservoir removed while buffer solution is being injected in order to displace as much trapped air as possible. The buffer reservoir is now completely full of fluid, and can be placed aside till needed. The pressure loader can be run till empty in order to free the capillaries of any fluid and simplify the identification of gel during gel injection, as outlined in the next step.

9.0 Second Iteration Results

With reworked tools created to isolate the crosstalk problem between neighboring capillaries, it was now necessary to design a series of experiments in order to properly isolate the crosstalk problem and its root cause. Two possible hypothesis were developed regarding the source of crosstalk: Either cross-microwell contamination was occurring during DNA injection at the bottom of the array, or the crosstalk is a result of migrating DNA once it had exited the top of the capillary array.

In order to test if the crosstalk was occurring at the bottom end of the capillary array, a 5 capillary x pattern was used instead of the entire 100 array. By using only 5 capillaries, no-cross contamination could be assured because of the lack of a capillary in a neighboring position to be contaminated. These experiments utilized the original buffer reservoir in order to keep all other variable constant. It was observed in this experiment (3-30) that crosstalk was less severe, there still was noticeable crosstalk in a pattern consistent with DNA drift in the fluid reservoir. These experimental results are shown in Figure 23 and 24.

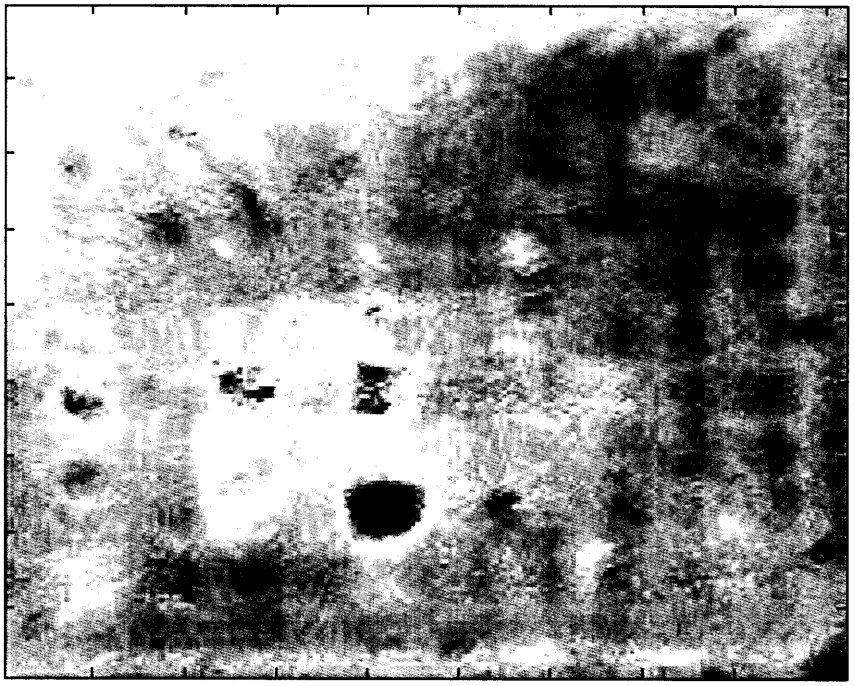

Figure 23: Crosstalk surrounding x-pattern within 100 capillary array (3-27-07).

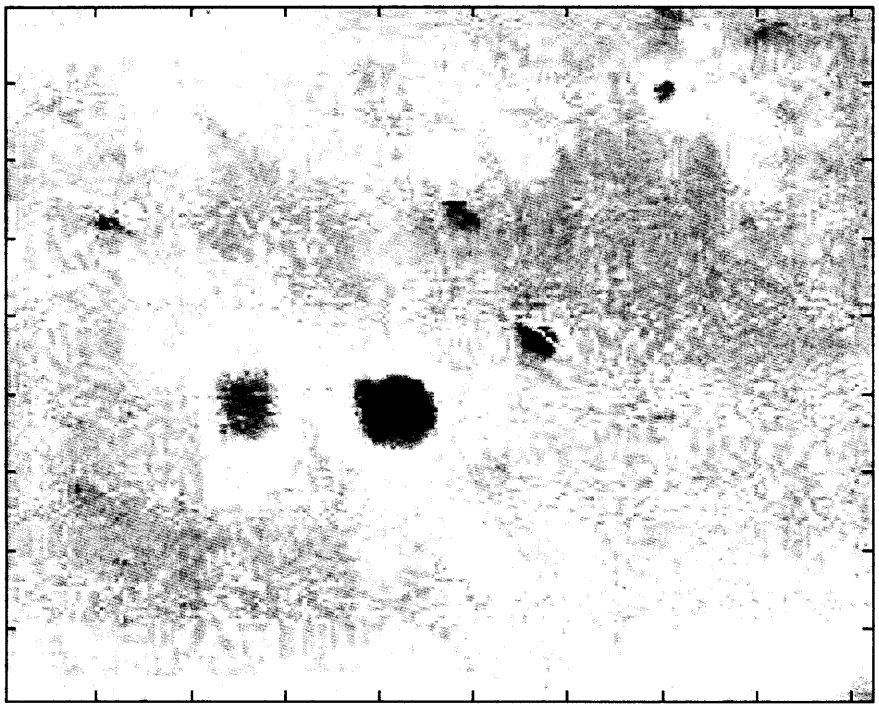

Figure 24: Crosstalk surrounding x-pattern with only 5 capillaries in array (3-30-07).

The results of these experiments validated that the crosstalk was occurring on the top end of the capillary array, since at this point there was not possible way for a neighboring capillary to have DNA, since no capillary existed in that position to begin with. The next step was to use the new buffer reservoir to attempt to isolate the signals on the top of the capillary array. The same parameters were used in the next experiment, except that longer 450 mm capillaries were substituted to allow for easier gel loading and DNA loading. Many of the previous experiments had been invalidated because of issued dealing with long exposure times to the air. Longer capillaries allowed for the use of the multi-capillary pressure gel loader as described in Nathan Ball's MIT Senior thesis [12] as a modular component separate from the thermal chamber mounting, as well as simplifying DNA injection from the microwell plate. The experiment was run with 200 nM solution to assure detection. The results of this next experiment are shown below in Figure 25.

Figure 25: New buffer reservoir initial trial, x-pattern (4-19-07).

The first trial using this new tool resulted in an unknown optical pattern being detected within the intended locations. A square was not observed, but rather two distinct points of high intensity. It was theorized that this may be due to an unfocused lens array. This trial had attempted to account for the movement of the array above the original focusing plane of the lenslet arrays. However, the calculated distance change of 1.6 mm turned out to be incorrect, resulting in this output pattern. The lens was then lowered to 1 mm above its original placement, and the experiment was run again at 200 nM to assure strong signal detection. Results are shown below in Figure 26.

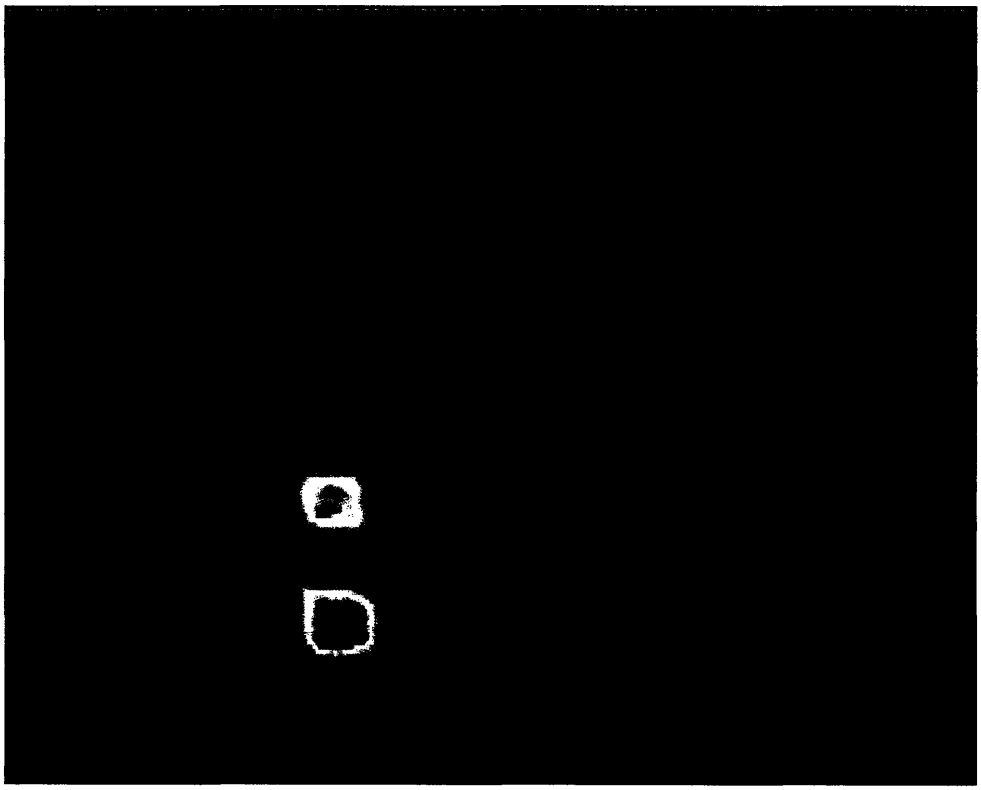

Figure 26: Corrected lens focusing distance, x-pattern (4-25-07).

This experiment shows the first successful complete isolation of the signal from neighboring capillaries. The correct focal length has allowed for CDCE end column detection using the new buffer reservoir, and avoiding accidental detection of DNA drift. Graphical data below shows the pixel intensity, with peaks reaching 800 counts above normal, indicating an extreme signal to noise ratio of 800:1.

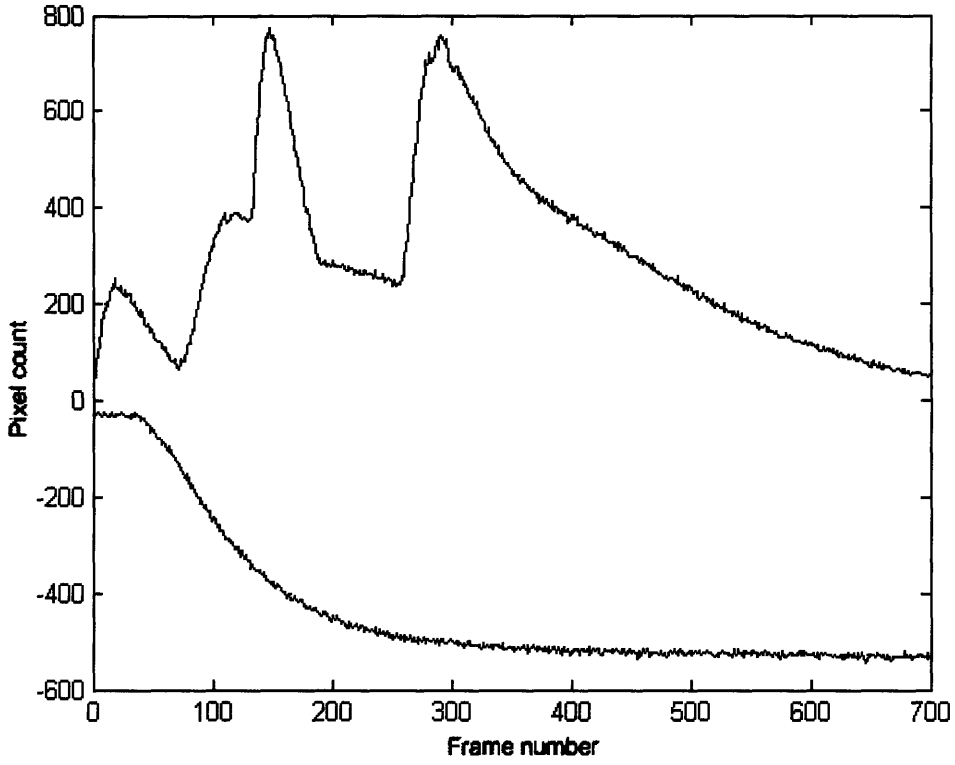

Figure 27: Maximum and Minimum pixel count data for relevant peaks during trial run (4-25-07).

This experiment was run at 200nM concentration, which is well above what is intended in the final UTMS device. The same experiment was then conducted with the correct 20 nM concentration primer solution. Results are shown below in Figure 28 and 29, displaying raw optical data and maximum and minimum pixel count data.

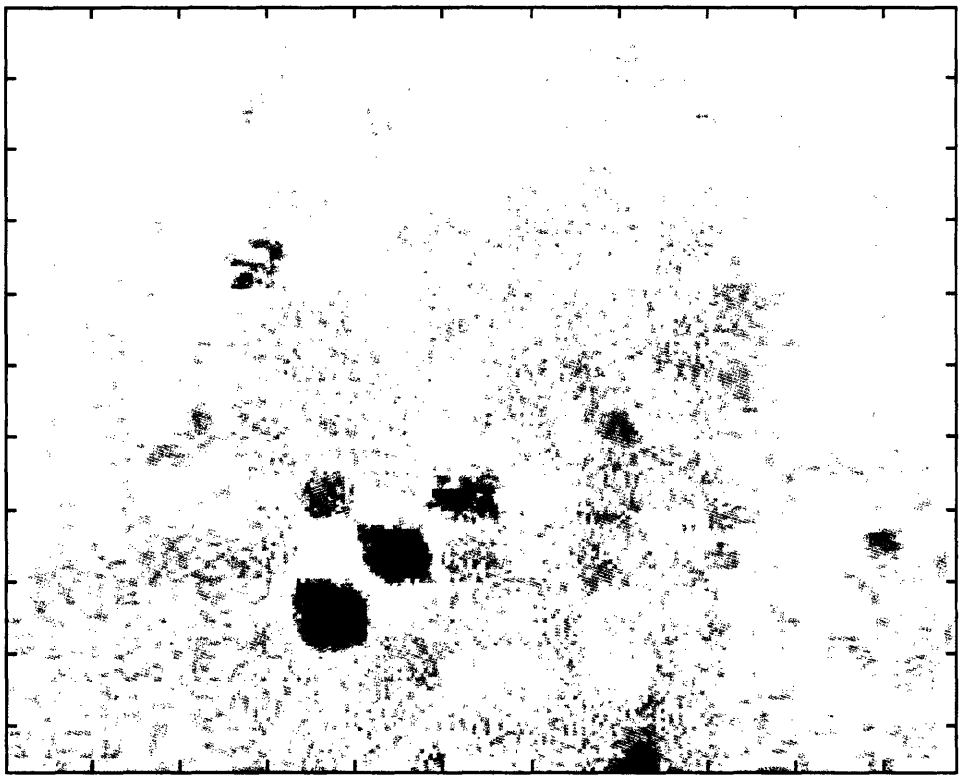

Figure 28: Lens focusing distance, x-pattern, 20 nM (4-26-07).

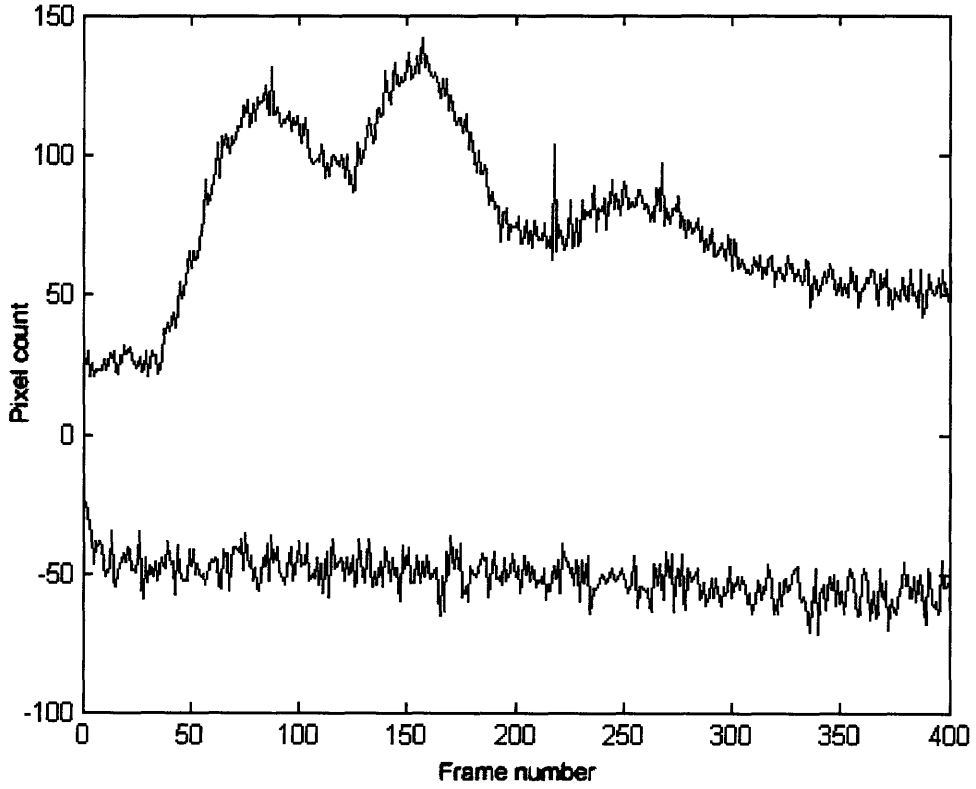

Figure 29: Maximum and Minimum pixel count data for relevant peaks during trial run (4-26-07).

The optical data again shows the lack of crosstalk in the x-pattern at 20 nM concentration, and pixel value count is shown to peak at approximately 150 counts, indicating a 150:1 signal to noise ratio, which is above the required 100:1 noise ratio as described in Forest *et al* [10]

Now that isolation has occurred on a small scale within the 100 capillary array, it is necessary to test the crosstalk with determined parameters with the entire 100 capillary array in place. The parameters chosen for this experiment were to inject alternating microwells with 20 nM DNA, to test as much possible crosstalk across the entire capillary array. Due to variations in capillary length, not all DNA primers emerged at the same instance in time. Shown below in figure 30 is the best frame which shows the most DNA signal at a given point in time, in addition to the maximum and minimum pixel count data.

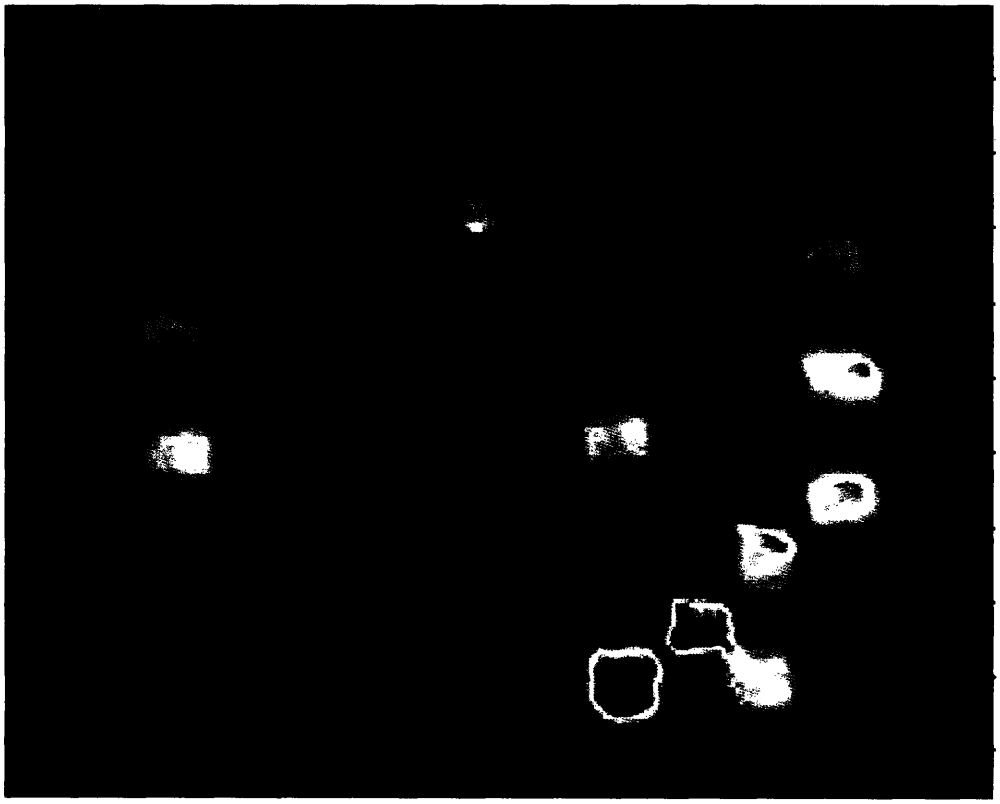

Figure 30: 100 capillary alternating injection pattern (5-3-07).

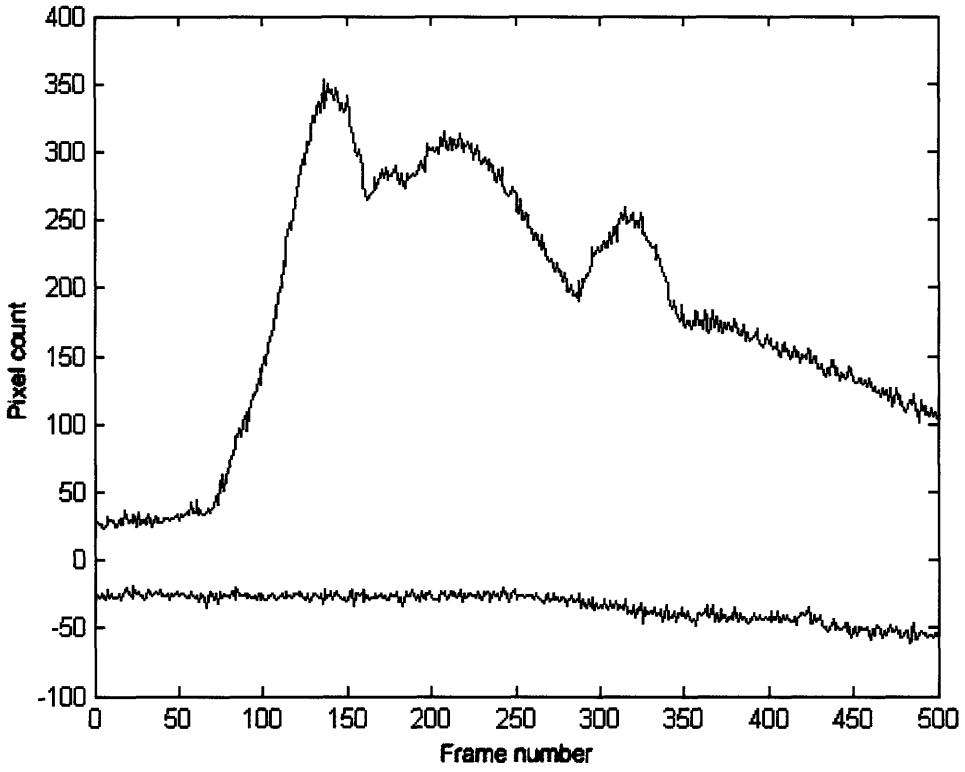

Figure 31: Maximum and Minimum pixel count data for relevant peaks during trial run (5-3-07).

This data shows a minimal amount of crosstalk occurring during the full 100 capillary array test. Much of this can be attributed to a minute drift observed in the lower pixel bound in Figure 30. The only obvious inconsistency is in the top left corner of the image, but this microwell was accidentally injected during the trial run, and was deemed acceptable in order to salvage the experiment. Thus, there is successful detection and signal isolation of the 100 capillary array alternating pattern at a 20 nM concentration.

10.0 Discussion

The tools necessary to conduct these experiments have also been designed and verified through experimentation, including two iterations of a top buffer reservoir, bottom buffer

reservoir, and DNA injection well. These new instruments now may work in conjunction with previously existing tools to run CDCE on the 100 capillary array within the UTMS instrument.

A system of procedures has also been developed which can be followed to avoid all of the problems associated with manually running CDCE on the 100 capillary array. This list of procedures has been experimentally verified to minimize the risk of invalid data, as well as prevent damage to sensitive components of the UTMS.

Isolation of each data channel has been successful through the use of a buffer reservoir which has allowed the detection plane to move above the fluid reservoir level, preventing the detection of drifting DNA which has previously exited the capillary array. The problem was isolated to the top section of the array through a series of experiments designed to isolate each possible cause and eliminate each variable one by one. The 100 capillary array has been shown to successfully display correct data, with no influence from neighboring capillaries.

10.1 Future Work

The next logical step in the 100 capillary proof of concept stage is the substitution of full DNA segments instead of DNA primers. This will require the use of the heat exchanger, which has been outlined in two previous MIT Bachelors of Science thesis reports [11,16] There has been extensive modifications made to the heat exchanger since the beginning of this thesis work, the control chamber will most likely require a verification of sealing, and incorporation of existing temperature sensors to verify the system operates within established parameters

One issue that may arise with the integration of the heat exchanger is the ambient heat put out by the system. A new procedure for cool-down and warm-up times may need to be derived,

since the cooling of the LED array may be significantly affected by the heat output of the thermal chamber.

Another concern is the viability of using the mechanisms in the buffer reservoir for capillary arrays over 100. While the technology is especially useful on the 100 capillary array, it requires a great deal of time and effort to ensure it is working properly. There is a "sweet spot" that can be hit, but a great number of factors can influence the alignment of the capillaries to the guide pins, and there is a significant learning curve to be able to confidently use the apparatus. Additionally, if the device is used incorrectly, repairs to the capillary array are difficult, but not impossible at this stage. There is easy access to capillaries within the outer 3 layers of the 10 × 10 array in the case that they are either broken or pushed into the constraint device, they can easily be accessed by pliers. However, once again there is a steep learning curve when learning the appropriate methods to fix the array without inflicting more damage. Additionally, repairs to the inner layers of the capillary array are difficult, as it becomes harder to access capillaries further away from the edges. If this technology were to be scaled up, there would be almost no chance of repairing a capillary more than 4-5 layers within the 100 × 100 array.

11.0 Conclusions

The 100-capillary proof of concept stage for the UTMS is now one step closer to completion. Successful detection of DNA primers has been accomplished, and the remaining step to achieve DNA mutation detection is merely a few experiments away. The tools and procedures developed to run CDCE on the 100 capillary array have been perfected, and successful signal isolation has been achieved. It is now possible to run experimentation on the 100 capillary array without fear of incorrect results from cross talk, with minimal risk of damage

from established procedures and use of universal passive alignment technology, and with the use of simple tools which provide the required electrical, optical, fluid components.

References

[1] Forest, C.R., Ball, N.B., So, P., Thilly, W.G., Hunter, I.W., 2006, *Two-dimensional capillary array electrophoresis end-column fluorescence detection*, Electrophoresis, (under revision)

[2] Morgenthaler, S., Thilly, W.G., 2005, *Summed multi-allelic risk: logical and a statistical models for discover of carrier genes in human populations*, Mutation Research, (submitted).

[3] Freeman, S. *Biological Science*, Prentice Hall, 2002.

[4] Cotton, R.G.H. *Mutation Detection*: Oxford University Press, 1997.

[5] Khrapko, K. Hanekamp, J. Thilly, W. Belenkii, A. Foret, F. Karger, B. *Constant denaturant capillary electrophoresis(CDCE). a high resolution approach to mutational analysis.* Nucleic Acids Research, 1994, Vol 22, No. 3, 364-369

[6] http://www.fermentas.com/catalog/electrophoresis/6xloadingsdsdye.htm

[7] C.R.Forest, *An Ultra-high Throughput Mutational Spectrometer for Human Genetic Diagnostics*, Doctoral Thesis, Department of Mechanical Engineering, MIT, May 2007

[8] Li-Sucholeiki, X. Khrapko, K. Andre, P. Marcelino, L. Karger, B. Thilly, W. *Applications of constant denaturant capillary electrophoresis/high-fidelity polymerase chain reaction to human genetic analysis.* Electrophoresis 1999, 20, 1224-1232.

[9] Khrapko, K. Coller, H. Andre, P. Li, X. Foret, F. Belenky. A. Karger, L. Thilly, W. *Mutational spectrometry without phenotypic selection: human mitochondrial DNA.* Nucleic Acids Research, 1997, Vol 25, No. 4. 685-693.

[10] C.R. Forest, N.B. Ball, T.A. Fofonoff, I.W. Hunter, *Two-Dimensional Capillary Array Electrophoresis End-Column Fluorescence Detection*, Proceedings of the 19th International Symposium on MicroScale Bioseparations (MSB) , p. 28, New Orleans, LA, February 12-17, 2005.

[11] Lin, Jiengju, J, *Manufacturing improvement and thermal property characterization of the frame structure of an Ultra-high throughput mutational spectrometer.* Bachelors of Science Thesis, Department of Mechanical Engineering, MIT, May 2005

[12] Ball, Nathan B., *Design and Characterization for a Gel Loading Mechanism for an Ultra-High Throughput Mutational Spectrometer.* Bachelors of Science Thesis, Department of Mechanical Engineering, MIT, June 2005

[13] C.R. Forest, B. Woodruff, I.W. Hunter, *Accurate, repeatable, and replaceable constraint of capillary arrays using a micro-fabricated device*, Proceedings of the 20th International

Symposium on MicroScale Bioseparations (MSB), p. 129, Amsterdam, Netherlands, January 22-26, 2006.

[14] C.R. Forest, B. Crane, I.W. Hunter, *Micro-well Array Interface for Capillary Array Electrophoresis*, Proceedings of the 9th International Conference on Miniaturized Chemical and Biochemical Analysis Systems (μTAS), V. 1, p. 141-144, Boston, MA, October 9-13, 2005.

[15] Slocum, A.H. 1992, *Precision Machine Design*, Prentice Hall, Inc.

[16] Suen, T. W., *Temperature Response of the Ultra-High Throughput Mutational Spectrometer*. Bachelors of science Thesis, Department of mechanical Engineering, MIT, June 2005

[17] Morgenthaller, S., Thilly, W., *A strategy to discover genes that carry milti-allelic or mono-allelic risk for common diseases: A cohort allelic sums test*, Mutation research [0027-5107] Morgenthaler yr:2007 vol:615 iss:1-2 pg:28 -56

Appendix A: Thermal control unit beam bending calculations

Shown is the beam bending equation for a simply supported beam

$$\delta = \frac{FL^3}{48EI},$$

(1)

where I is polar moment of inertia of a rod, F is applied force, L is length of the rod, E is the modulus of elasticity of steel, and δ is deflection. I is given by:

$$I = \frac{\pi D^4}{64}.$$

(2)

Substituting in to equation 1 and solving for D,

$$D^4 = \frac{64FL^3}{48E\pi\delta}.$$

(3)

Substituting in givens and constants to Equation 3: F = 500 N (assumed weight of thermal control chamber with water), L = 0.6096 m, E = 1.93×10^{11} kg/ms^2, and maximum allowable deflection δ = 1mm

$$D = \left[\frac{(64)(500N)(0.6096m)^3}{(48)(1.93\times10^{11})(\pi)(1mm)}\right]^{\frac{1}{4}} = 0.016m$$

(4)

Appendix B: System Error Budget for Buffer Reservoirs

Error Gain Spreadsheet — Written by Alex Slocum, John Moore, Whit Rappole October 4, 1999

Buffer Resevoir Error Analysis

Nominal coordinate values		Sum Random Errors in the reference CS		RSS Random Errors in the reference CS		Average SUM & RSS random errors in the reference CS		Net Total Systematic Errors in the reference CS	
X=	0.0000	δX=	0.3806	δX=	0.2149	δX=	0.2978	δX=	0.0000
Y=	0.0000	δY=	0.3806	δY=	0.2149	δY=	0.2978	δY=	0.0000
Z=	-4.8100	δZ=	0.0406	δZ=	0.0354	δZ=	0.0380	δZ=	0.0000
		εX (rad) =	0.0007	εX (rad) =	0.0006	εX (rad) =	0.0007	εX (rad) =	0.0000
		εY (rad) =	0.0007	εY (rad) =	0.0006	εY (rad) =	0.0007	εY (rad) =	0.0000
		εZ (rad) =	0.0000	εZ (rad) =	0.0000	εZ (rad) =	0.0000	εZ (rad) =	0.0000

Enter numbers in BOLD Output is in RED

Number, N, of coordinate systems (not including the reference system) MAXIMUM OF 15	Systematic errors: systematic	thermal	dynamic
8	on	off	off

CS #	Description:	Capillary Tip				
8	All errors for this axis on/off			on		
Axes	Actual dimensions	Random errors	systematic	thermal	dynamic	Error descriptions
X	0	0.1940	0.0000	0.0000	0.0000	x,y error due to protrusion of capillary measurements (craig, nov 2005)
Y	0	0.1940	0.0000	0.0000	0.0000	x,y error due to protrusion of capillary measurements (craig, nov 2005)
Z	-11.07	0.0000	0.0000	0.0000	0.0000	
θX (rad)	0	0.0000	0.0000	0.0000	0.0000	
θY (rad)	0	0.0000	0.0000	0.0000	0.0000	
θZ (rad)	0	0.0000	0.0000	0.0000	0.0000	

CS #	Description:	Silicone Constraint				
7	All errors for this axis on/off			on		
Axes	Actual dimensions	Random errors	systematic	thermal	dynamic	Error descriptions
X	-15.5	0.0650	0.0000	0.0000	0.0000	capillary moving within allowance of square steel hole (capillary in silicone)
Y	-15.5	0.0650	0.0000	0.0000	0.0000	capillary moving within allowance of square steel hole (capillary in silicone)
Z	0	0.0000	0.0000	0.0000	0.0000	
θX (rad)	0	0.0000	0.0000	0.0000	0.0000	
θY (rad)	0	0.0000	0.0000	0.0000	0.0000	
θZ (rad)	0	0.0000	0.0000	0.0000	0.0000	

CS #	Description:	Constraint Plate				
6	All errors for this axis on/off			on		
Axes	Actual dimensions	Random errors	systematic	thermal	dynamic	Error descriptions
X	-10	0.0000	0.0000	0.0000	0.0000	RSS of milling machine tolerance and clearance hole allowance of 0.1 mm
Y	20	0.0000	0.0000	0.0000	0.0000	RSS of milling machine tolerance and clearance hole allowance of 0.1 mm
Z	-0.3	0.0000	0.0000	0.0000	0.0000	
θX (rad)	0	0.0000	0.0000	0.0000	0.0000	
θY (rad)	0	0.0000	0.0000	0.0000	0.0000	
θZ (rad)	0	0.0000	0.0000	0.0000	0.0000	

CS #	Description:	Top Cover Plate				
5	All errors for this axis on/off			on		
Axes	Actual dimensions	Random errors	systematic	thermal	dynamic	Error descriptions
X	-13	0.0200	0.0000	0.0000	0.0000	milling machine accuracy determines hole placement
Y	-22	0.0200	0.0000	0.0000	0.0000	milling machine accuracy determines hole placement
Z	0	0.0000	0.0000	0.0000	0.0000	gasket thickness (z dimension)
θX (rad)	0	0.0000	0.0000	0.0000	0.0000	
θY (rad)	0	0.0000	0.0000	0.0000	0.0000	
θZ (rad)	0	0.0000	0.0000	0.0000	0.0000	

CS #	Description:	Dowel pins				
4	All errors for this axis on/off			on		
Axes	Actual dimensions	Random errors	systematic	thermal	dynamic	Error descriptions
X	0	0.0500	0.0000	0.0000	0.0000	accuracy of placement and oversized acrylic holes
Y	0	0.0500	0.0000	0.0000	0.0000	accuracy of placement and oversized acrylic holes
Z	8.96	0.0000	0.0000	0.0000	0.0000	
θX (rad)	0	0.0001	0.0000	0.0000	0.0000	pin doesn't stick straight up
θY (rad)	0	0.0001	0.0000	0.0000	0.0000	pin doesn't stick straight up
θZ (rad)	0	0.0000	0.0000	0.0000	0.0000	

CS #	Description:	BR - 2nd Alignment Plate				
3	All errors for this axis on/off			on		
Axes	Actual dimensions	Random errors	systematic	thermal	dynamic	Error descriptions
X	38.5	0.0200	0.0000	0.0000	0.0000	
Y	17.5	0.0200	0.0000	0.0000	0.0000	
Z	0	0.0000	0.0000	0.0000	0.0000	
θX (rad)	0	0.0006	0.0000	0.0000	0.0000	0.05/80 allowable rotation
θY (rad)	0	0.0006	0.0000	0.0000	0.0000	0.05/80 allowable rotation
θZ (rad)	0	0.0000	0.0000	0.0000	0.0000	

CS #	Description:	BR - Silcone Seal				
2	All errors for this axis on/off			on		
Axes	Actual dimensions	Random errors	systematic	thermal	dynamic	Error descriptions
X	0	0.0000	0.0000	0.0000	0.0000	
Y	0	0.0000	0.0000	0.0000	0.0000	
Z	-0.5	0.0000	0.0000	0.0000	0.0000	
θX (rad)	0	0.0000	0.0000	0.0000	0.0000	
θY (rad)	0	0.0000	0.0000	0.0000	0.0000	
θZ (rad)	0	0.0000	0.0000	0.0000	0.0000	

CS #	Description:	BR - 1st Alignment Plate				
1	All errors for this axis on/off			on		
Axes	Actual dimensions	Random errors	systematic	thermal	dynamic	Error descriptions
X	0	0.0290	0.0000	0.0000	0.0000	rss of 0.02 (milling accuracy) and (.381-.360=.021) cap clearance in hole
Y	0	0.0290	0.0000	0.0000	0.0000	rss of 0.02 (milling accuracy) and (.381-.360=.021) cap clearance in hole
Z	-1.9	0.0000	0.0000	0.0000	0.0000	
θX (rad)	0	0.0000	0.0000	0.0000	0.0000	
θY (rad)	0	0.0000	0.0000	0.0000	0.0000	
θZ (rad)	0	0.0000	0.0000	0.0000	0.0000	

Appendix C: Matlab image analysis code

```
%craig forest, michael beltran

%create modified file of "make_image_seq_movie.m" to use imagesc
     function
%to attempt to improve RAM usage and calculation times.

warning off;
clc;
clear all;
close all;

%First and last image to examin in sequence
first=700;
last=1100;
clim_cutoff=0;

colornum=8;
colormap(hsv(2^colornum));

%this section of code creates selects a value to establish a
     common
%background for all frames.  first a 10*10 box is selected, then
     all pixels
%within that box are averaged to get a background reading for
     that frame.
%The highest background is selected and then all frames are
     biased to have
%that background intensity
%specify 10x10 box where intensity will be constant
pospivoty=10; %60;
pospivotx=10; %80;
sizepivotbox=10; %10;

for p=first:last;
    if p<10;
        singledigs=strcat('00',num2str(p));
        filename=strcat('Image-',num2str(singledigs),'R.tif');
        img=imread(filename);
    elseif p<100;
        doubledigs=strcat('0',num2str(p));
        filename=strcat('Image-',num2str(doubledigs),'R.tif');
        img=imread(filename);
    else
        filename=strcat('Image-',num2str(p),'R.tif');
        img=imread(filename);
    end
    img_math = double(img) + 1;  %so that math can be done on
     the image matrix
```

```
     img_pivot_values=img_math(pospivotx:pospivotx+sizepivotbox,p
     ospivoty:pospivoty+sizepivotbox);
    img_pivot_mean=mean(mean(img_pivot_values));


    if p==first
        ref=img_math;
        prefmean=img_pivot_mean;
        [l,w]=size(ref);
        imgseq=zeros(l,w,last-first);
        matrix_ind=(last-first)*l*w;
    else
        A=img_math;
        pimgmean=img_pivot_mean;
        A2=A-(pimgmean-prefmean);
        A3=A2-ref;
        imgseq(:,:,p-first)=A3;
   p
%         image(A3)
%         p
%         Q(p-first)=getframe;

    end

end

for m=first:last
    if m==last
    else
    minvect(m-first+1)=min(min(imgseq(:,:,m-first+1)));
    maxvect(m-first+1)=max(max(imgseq(:,:,m-first+1)));
    end
end
clc;
matrix_ind
plot(minvect)
hold on
plot(maxvect)
% movie(Q);

lower_offset=min(minvect);
upper_offset=max(maxvect);
clims=[1 upper_offset-lower_offset-clim_cutoff];
tic
imgseq2=imgseq-lower_offset;
toc
figure
for n=first:last-1
    imagesc(imgseq2(:,:,n-first+1),clims)
    colorbar
    title(sprintf('imagenum=%d',n));
```

```
    Q(n-first+1)=getframe;
    %pause
end
%
movie(Q)
movie2avi(Q,'movie.avi')
```